

# A Framework for Stochastic Air Traffic Flow Modeling and Analysis

P. K. Menon<sup>1</sup>, Monish D. Tandale<sup>2</sup>, Jinwhan Kim<sup>3</sup>, and Prasenjit Sengupta<sup>4</sup>  
*Optimal Synthesis Inc, Los Altos, CA, 94022- Control ID 814153*

**A framework for stochastic traffic flow modeling over the U. S. National airspace based on queuing network models is advanced. The proposed framework allows the inclusion of a wide variety of trajectory uncertainties such as delays due to weather deviation, air traffic control actions, en route wind, aircraft performance, navigation system precision and flight control. En route queuing networks models are developed at origin-destination airport-level, Center-level, Sector-level and Latitude/Longitude-level spatial resolutions. Queuing models for the taxi, runway and TRACON flight segments have also been developed. Two approximations are employed to derive closed-form solutions to the queuing networks. Comparisons with Monte Carlo simulations and historic traffic data are used to validate the queuing network models. Validated queuing network models are then used to analyze a few next-generation air traffic operations concepts. The present research demonstrates that queuing network model solutions can closely approximate the Monte Carlo simulations, while delivering results at substantial savings in computational effort.**

## I. Introduction

A detailed understanding of the relationship between trajectory uncertainties due to aviation operations, precision of navigation and control, and the traffic flow metrics is essential for designing next-generation air transportation system. A well-known approach to stochastic analysis of complex dynamic systems is through Monte Carlo simulations. For instance, Monte Carlo simulation methodology with National Airspace System (NAS) air-traffic simulation programs such as FACET<sup>1</sup> and ACES<sup>2</sup> can be used to quantify stochastic effects. However, these simulations can consume enormous amounts of time and are not easily amenable for use in conducting rapid trade studies. On the other hand, certain formulations of queuing network models<sup>3</sup> of the air traffic system can provide explicit relationships between traffic flow efficiency and trajectory uncertainties, facilitating tradeoff studies in an effective and time-efficient manner. Complexity of this analysis depends upon the type of the queuing network employed. For instance, Markovian queuing networks<sup>4</sup> can provide fast solutions at lower fidelities of traffic flow representation, while Coxian queuing networks<sup>5</sup> can represent complex traffic phenomena at higher fidelities with the attendant increase in computational effort. The intermediate QNA approximation<sup>6</sup> provides moderate-fidelity results, at slightly more computational effort than the Markovian networks. Figure 1 illustrates the Fidelity-Computational Effort tradeoffs in the stochastic analysis of the NAS traffic flow. When properly formulated, queuing networks can provide high-quality stochastic results, often approaching the accuracies delivered by Monte Carlo simulations. This fact will be illustrated in one of the following sections.

Queuing models are one of the earliest developments in the now well-established field of Operations Research. According to Reference 3, much of this theory is attributed to the early works of Erlang<sup>7</sup> on the problems in telephony. Although most of applications continued to be in telephony and surface transportation, post-second World War surge in aviation lead to several applications of the queuing theory for the study of air traffic<sup>8-10</sup>. Since then, this modeling methodology has been successfully adopted for addressing various aspects of the aviation system by the airlines, air cargo fleet operators, and air traffic control system designers. A recent example of the queuing network model of the NAS can be found in Reference 11.

---

<sup>1</sup> Chief Scientist, 95 First Street, Suite 240, Fellow AIAA.

<sup>2</sup> Research Scientist, 95 First Street, Suite 240, Member AIAA.

<sup>3</sup> Research Scientist, 95 First Street, Suite 240, Senior Member AIAA. Presently: Assistant Professor, Korea Advanced Institute of Science and Technology, Daejeon 305-701, Republic of Korea.

<sup>4</sup> Research Scientist, 95 First Street, Suite 240, Senior Member AIAA.

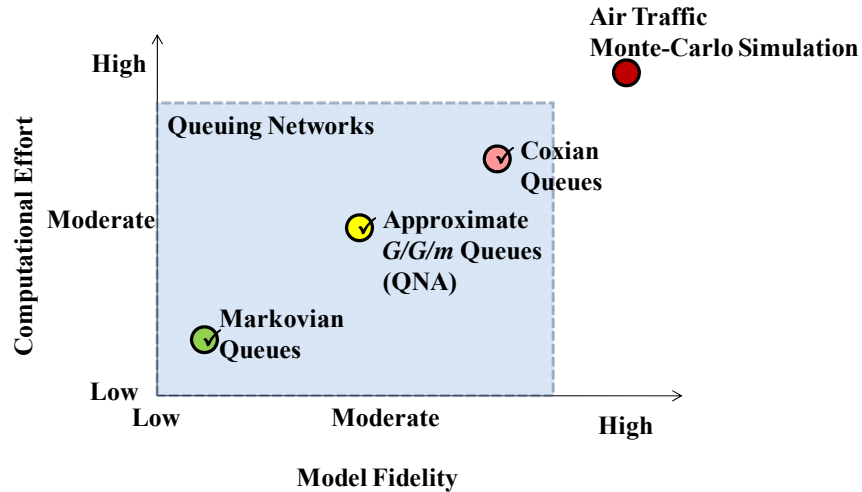


**Figure 1. Comparison between approaches for the Stochastic Analysis of the National Airspace System**

Although several air traffic queuing models have been described in the literature, none of them have included the effects of trajectory uncertainties due to aviation operations and precision of navigation and control on the traffic flow efficiency. Moreover, general approaches for developing comprehensive queuing network models of the NAS have not been discussed in the published literature. These are the central issues addressed in the present research. Major factors contributing to the trajectory uncertainties and precision are illustrated in Figure 2.

Some of these uncertainties influence the climb and descent flight segments, while others predominantly affect the cruise flight segment. For instance, aircraft performance in climb and descent are uncertain due to variations in weight, power plant, aerodynamics, atmospheric density, and Terminal Radar Approach Control (TRACON) operations. Ambient winds, navigation systems and flight plan deviations due to air traffic management and weather are major contributors to cruise uncertainties. Detailed uncertainty models relating these factors, and the methods for integrating the uncertainties into the nominal queuing models are some of the objectives of the present paper.

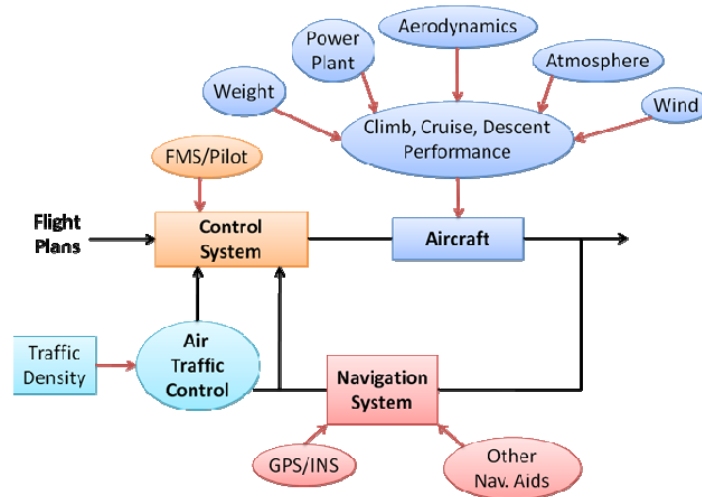


**Figure 2. Factors Contributing to Trajectory Uncertainty**

The operating characteristics of queuing systems are mainly determined by three statistical properties, namely, the probability distribution of inter-arrival times and the service times<sup>3,18</sup>

<sup>19</sup>, and the mean flow fractions<sup>4</sup> between queuing network nodes. These distributions can take almost any form in real queuing systems. The complexity in deriving queuing solutions

depends upon the form of the inter-arrival and service time distributions. For instance, if these distributions are exponential, the NAS can be modeled as an open Jackson network<sup>4</sup>

<sup>19</sup>, allowing the computation of queuing results using simple algebraic formulas. Queues with exponential inter-arrival and service time distributions are termed as Markovian queues. Note that the exponential service time distribution allows a very high degree of variability. Most of the queuing results in the literature are given for steady-state Markovian queues with time-invariant inter-arrival and service time distributions.

If the inter-arrival and service time distributions are not exponential, the solution process will require the formulation of the Chapman-Kolmogorov equation based on exhaustive state-enumeration

<sup>19</sup>, followed by the numerical solution of a large system of linear differential equations. Due to the extreme dimensions of the resulting state space, often, solutions can only be obtained through decomposition methods<sup>5</sup>. For systems with small number of states, the state-enumeration methodology can be used to generate transient behavior of the queues. Moreover, the methodology can be employed for systems with time-varying distributions. Nevertheless, this approach is not computationally feasible for systems with very large number of states.

Due to these reasons, it is customary to initially create models based on the Markov assumption and subsequently refine them to include finer details. While all the details of the air traffic flow in the NAS cannot be completely captured using such grossly simplified stochastic models, Markovian results can serve as the baseline for more sophisticated queuing models incorporating more general inter-arrival and service distributions.

As an aside, the aggregate traffic flow models discussed in the recent literature<sup>12-17</sup> can be considered to be special forms of the queuing network models. The chief difference between them is that while queuing networks focus on the steady-state stochastic behavior of time of arrival and transit through the system, the aggregate models in References 12 - 17 focus on temporal evolution of aircraft counts in the airspace. In addition to being useful for transient analysis of air traffic flow, aggregate models can also be used to create stochastic analysis of the traffic flow as indicated in Reference 14, with time as the independent variable. At identical spatial resolutions, it can be shown that the mean traffic flow rates from the queuing network and the aggregate models in References 12 - 14 will be equal.

## II. Queuing Network Models of the National Airspace System

The queuing network abstraction of the NAS is illustrated in Figure 3. The colored circles in the figure represent service components, and the blue-red accordion structures illustrate the regions in which "queues" can form by aircraft waiting for service.

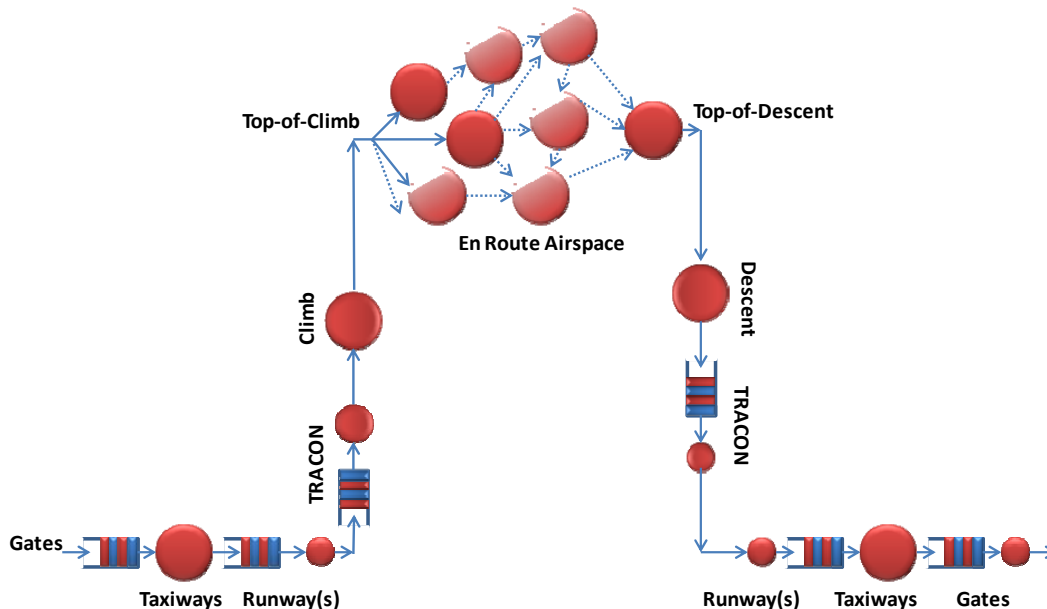


Figure 3. Queuing Network Abstraction of the National Airspace System

After being pushed back from the departure gates, the aircraft may have to wait to begin their taxi operation or being "served" by the taxiways. Upon reaching the runway, the aircraft may once again have to wait to be served by

the runways for takeoff. In congested airspace, the aircraft may have to wait in the TRACON in "queues" before climbing out to the cruise altitude at the top-of-climb. The aircraft streams may then split-off in different directions depending on their destinations. Flow fractions define the proportions of aircraft streams branching-off in various directions, to be "served" by the en-route airspace.

The en-route airspace is generally discretized into service areas. For instance, the airspace may be discretized based on Air Route Traffic Control Centers (ARTCC) or air traffic control Sectors. Other possible discretization schemes include origin-destination pair-wise representation of the airspace, or the more general latitude-longitude tessellation described in Reference 14.

A reverse of the climb sequence occurs upon aircraft arrival at their destinations. Aircraft streams from different directions merge at the top-of-descent before being served by the descent airspace, perhaps followed by waiting in "queues" in the descent TRACON. After being "served" by the runway, the aircraft may then have to wait in queues before being served the taxiways, and finally the gates.

As can be observed from these discussions, the queuing network model captures the statistics of the traffic flow through a compact set of parameters. The use of these parameters to carry out stochastic analysis of the air traffic flow will be illustrated in one of the following sections.

### A. Computing the Parameters of Airspace Queuing Networks

The parameters of the queuing network describing the air traffic flow in the NAS can be computed using historic data. For the present work, daily air traffic data for the year 2007 from Aircraft Situation Display to Industry (ASDI) data feed from the FAA is used to generate the queuing network parameters. The ASDI data contains the position and time stamp for every flight operating on a given day. This data is used to generate input files for FACET. FACET simulations are then carried out to obtain aircraft track data at close intervals. The set of trajectories from FACET forms the input data for the computation of the queuing network parameters.

The inter-arrival times at the airports, the service times through the discretized airspace, and flow fractions at the network nodes can be determined by following a bookkeeping procedure to create histograms of data. These histograms can then be approximated to create the probability density functions for use in the queuing network models. As an example, Figure 4 illustrates the inter-arrival time distribution of air traffic into the NAS for a specific day in 2007, as well as for the entire year.

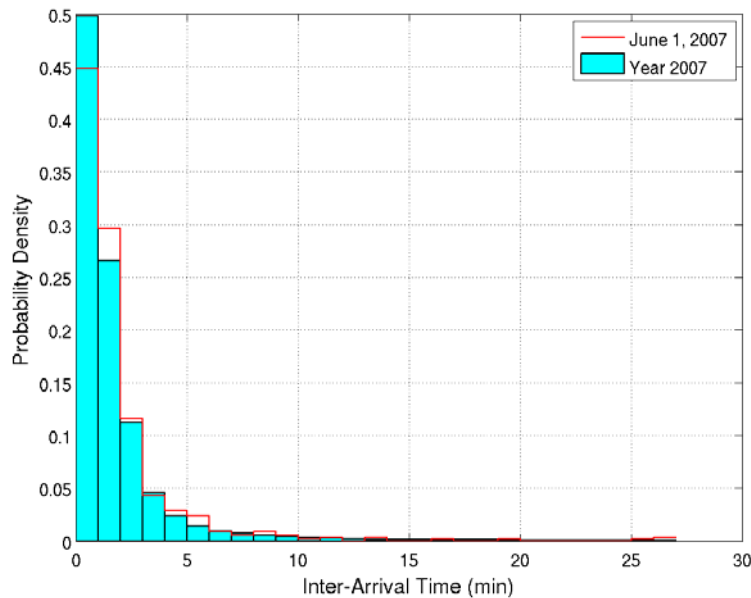
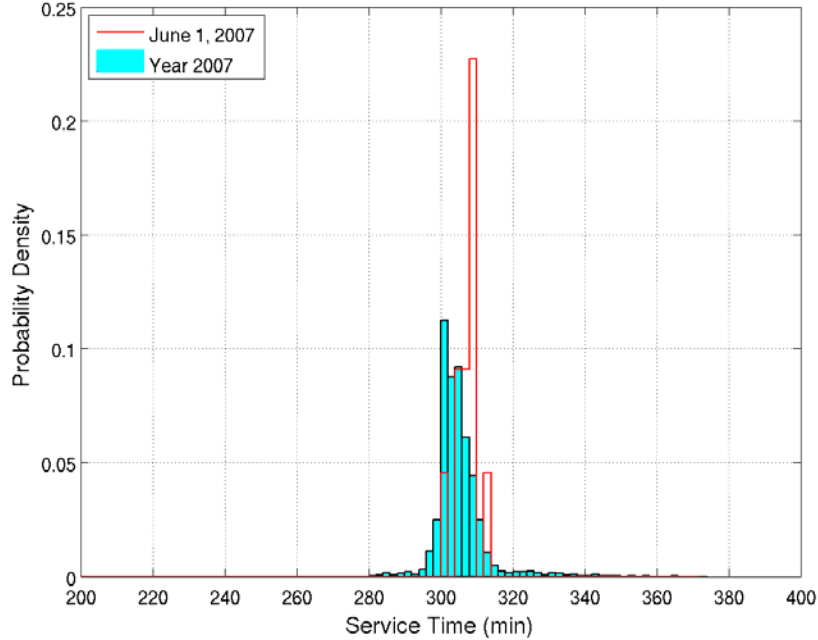


Figure 4. Inter-Arrival Time Distribution of Flights into the Network, from Phoenix (KPHX)

Figure 5 illustrates the service time distribution for flights traveling between Los Angeles International Airport (KLAX) and the New York's John F. Kennedy International airport (KJFK) for a specific date in 2007 and for the entire year.



**Figure 5. Service Time Distribution between Los Angeles International (KLAX) and John F. Kennedy International (KJFK) Airports**

It may be observed from these figures that the inter-arrival times are well approximated by exponential distributions. However, the service time distributions tend to be much more complex.

A software package termed AQUS (Airspace Queuing System) has been developed to automatically reduce a given ASDI data set into queuing network parameters. The AQUS software can be used in conjunction with interactive scripting environments to derive data for formulating the airspace queuing network models and to generate solutions. The interface is particularly useful for the analysis of traffic flow metrics in a visual or numerical format. Moreover, the AQUS software can readily be accessed by scripts written in popular computational platforms.

## **B. Uncertainty Models for Queuing Analysis**

In addition to the normal variability of traffic flow, aircraft operations are characterized by uncertainties induced by several other factors. These were illustrated in Figure 2. The objective of the uncertainty modeling process is to determine the impact of various uncertainties on the service times in the queuing network models. Models of some of these uncertainties will be discussed in this section. Since the en-route segment forms the largest portion of the flight time in long-haul routes, the focus of the present discussions will be on en-route uncertainty models. Three en-route uncertainty components will be presented. A more detailed discussion of the uncertainty models for air traffic flow analysis can be found in Reference 20.

### *Trajectory Uncertainty due to Navigation and Control*

Modern aircraft navigation requires accurate and reliable position/velocity estimates of the vehicle. Consequently, the sensor uncertainty and the sensor-induced control uncertainty will impact aircraft service time in the airspace. The navigational information is derived from onboard navigation sensors and external telemetry systems such as VOR/DME and GPS. In general, the navigation data is corrupted by measurement noise. This introduces uncertainty in the sensor outputs, and aircraft control based on this noise-corrupted sensor information induces additional uncertainties.

A simplified 1-D dynamic model of the aircraft is considered for the present uncertainty modeling. This model is represented as a two-state system consisting of the aircraft position  $x$ , aircraft speed  $v$ , driven by a random acceleration  $n_v$ :

$$\begin{bmatrix} \dot{x} \\ \dot{v} \end{bmatrix} = \begin{bmatrix} 0 & 1 \\ 0 & 0 \end{bmatrix} \begin{bmatrix} x \\ v \end{bmatrix} + \begin{bmatrix} 0 \\ n_v \end{bmatrix} \quad (1)$$

The random acceleration term,  $n_v \sim N(0, \sigma_v^2)$ , is assumed to be white-Gaussian, approximating the uncertainty from the onboard inertial sensor system (INS/IRS/IMU). The resulting position error is a random walk process. Periodic position fix inputs are used to correct the drift in the random walk process. Although VOR/DME has traditionally been used for aircraft navigation, the recent trend has been to move towards the use of GPS for obtaining the position fixes. A position fix measurement model can be represented using a measurement model:

$$z = \begin{bmatrix} 1 & 0 \end{bmatrix} \begin{bmatrix} x \\ v \end{bmatrix} + n_x \quad (2)$$

The measurement noise  $n_x \sim N(0, \sigma_x^2)$  is also assumed to be white-Gaussian. This model can be used to formulate an algebraic Riccati equation<sup>21</sup> that provides the error covariance matrix due to sensor process and sensor noise components as:

$$0 = AP + PA^T + Q - PH^T R^{-1} HP \quad (3)$$

The solution to this equation can then be obtained as:

$$P_{ss} = \begin{bmatrix} P_{11} & P_{12} \\ P_{21} & P_{22} \end{bmatrix} = \begin{bmatrix} \sqrt{2\sigma_x^3\sigma_v} & \sigma_x\sigma_v \\ \sigma_x\sigma_v & \sqrt{2\sigma_x\sigma_v^3} \end{bmatrix} \quad (4)$$

A similar approach is used to model the uncertainties due to flight control. Most modern commercial aircraft are equipped with the flight management system (FMS) and one or more autopilots. Control inputs commanded by the autopilot are calculated based on the state estimate containing navigational uncertainty errors. Hence, the sensor uncertainty components are fed-back into the system through the feedback control loop, and causes additional output uncertainty. Linear dynamics and measurement equations of the following form are assumed to model aircraft under control:

$$\dot{x} = Ax + Bu + n_x \quad (5)$$

$$z = Hx + n_z \quad (6)$$

where  $n_x \sim N(0, r_x)$  and  $n_v \sim N(0, r_v)$ .

The state estimate generated by the Kalman filter in the navigation loop is represented as

$$\dot{\hat{x}} = A\hat{x} + Bu + PH^T R^{-1}(z - H\hat{x}) \quad (7)$$

The FMS/autopilot control input is expressed as:

$$u = -K\hat{x} \quad (8)$$

The feedback gain  $K$  is chosen to yield time constants comparable to typical transport aircraft. Feedback control law can be substituted in the state estimator (7) to yield

$$\dot{\hat{x}} = (A - BK)\hat{x} + PH^T R^{-1}(z - H\hat{x}) \quad (9)$$

Or

$$\dot{\hat{x}} = (A - BK)\hat{x} + PH^T R^{-1}\tilde{z} \quad (10)$$

As in the case of navigation errors, an algebraic Riccati equation can be formulated for control uncertainties as:

$$0 = (A - BK)\hat{P} + \hat{P}(A - BK)^T - PH^T R^{-1} HP \quad (11)$$

The solution to Equation (12) can then provide the uncertainties due to control. Nominal input parameter values for modeling sensor uncertainties are determined considering physically reasonable sensor error characteristics given in Table 1. This data is derived from References 22 and 23.

Based on these parameter settings, internal parameter values such as the autopilot gain setting and manual flight control uncertainty for setting up the proposed simplified sensor error model can be calculated. The uncertainty contribution due to either autopilot or manual flight control is estimated based on the given accuracy information in Table 1. Note that the control gains are determined by assuming that the system is critically damped. The resulting position and velocity uncertainties are parameterized as  $\sigma_{pos}$  and  $\sigma_{spd}$ , respectively. The results are presented in Table 2.

**Table 1. Sensor/Control Parameter Settings**

Parameter	Value	Remark
System Dynamics Update Frequency	100 (Hz)	i.e.) INS update frequency
Position Fix Updated Frequency	1 (Hz)	i.e.) GPS update frequency
IRS drift (95%)	6*T (NM)	0 < T < 0.67, T in hours
IRS/GPS Position Accuracy (ANP: Rayleigh Distribution)	0.1 (NM)	w/ Dual FMC
Flight Technical Error (95% ) Autopilot	0.055 (NM)	LNAV with Autopilot Coupled
Flight Technical Error (95%) Manual Control	0.208 (NM)	Manual Flight with Map Display

**Table 2. Uncertainties due to Navigation Sensor and Flight Control**

	Speed deviation $\sigma_{spd}$ (kts)	Position deviation $\sigma_{pos}$ (ft)
Sensor Uncertainty Only	3.57	248.3
w/ Auto-pilot	6.46	283.4
w/ Manual Flight Control	22.4	573.1

The next step in the uncertainty modeling process is that of transforming the error components in the preceding tables into uncertainties in service time. Service time is defined as the time interval for an aircraft to traverse a given airspace. The nominal service time can be calculated by dividing flight distance by the nominal aircraft speed. However, the actual service time varies due to the presence of navigation errors and other uncertainties. Aircraft are controlled based on navigation sensor information provided to the autopilot or the human pilot. Navigational uncertainties will cause variations in speed, heading and flight path angles. Speed variation due to navigation uncertainty can either increase or reduce the service time. However, heading/flight angle deviations will always increase the service time, since the effective flight path is stretched by any deviations from the great-circle air route.

The kinematic equations of motion for a point-mass aircraft model in 3-D configuration space are:

$$\dot{x} = V \cos \gamma \cos \chi, \quad \dot{y} = V \cos \gamma \sin \chi, \quad \dot{h} = V \sin \gamma \quad (12)$$

where  $V$  is the aircraft speed,  $\gamma$  is the flight angle, and  $\chi$  is the heading angle. Assuming that the desired trajectory is directed along the downrange  $x$  direction, and that a feedback control system maintains the cross range  $y$  and the altitude deviation  $h$  close to zero, the cross-range/altitude dynamics can be expressed as:

$$\dot{y} = -k_y y, \quad \dot{h} = -k_h h \quad (13)$$

Substituting these in (14), and solving for the flight path angle and heading angle yields:

$$\cos \gamma = \sqrt{\frac{V^2 - k_h^2 h^2}{V^2}}, \quad \cos \chi = \sqrt{\frac{V^2 - k_y^2 y^2 - k_h^2 h^2}{V^2 - k_h^2 h^2}} \quad (14)$$

Thus, the effective speed along path can be expressed as:

$$\dot{x} = \frac{dx}{dt} = \sqrt{V^2 - k_y^2 y^2 - k_h^2 h^2} \quad (15)$$

The service time can be obtained by integrating the reciprocal of the expression in Equation (16):

$$t_f = \int_0^{x_f} \frac{1}{\dot{x}} dx = \int_0^{x_f} \frac{1}{\sqrt{V^2 - k_y^2 y^2 - k_h^2 h^2}} dx \quad (16)$$

For deterministic systems, the evaluation of the above expression involves a quadrature. However, since the variables  $V$ ,  $y$ , and  $h$  in the integrand in the above equation are random variables, the distribution for  $t_f$  needs to be calculated through stochastic integration.

Exhaustive approaches based on Monte Carlo integration techniques can be employed for the stochastic integration. However, the present approach is to develop analytical or semi-analytical techniques that can provide a close approximation to the Monte Carlo simulation results is outlined in Reference 20. That work shows that approximate service time distribution due to navigation and control uncertainties can be expressed as:

$$f_{T(x)}(t) = \frac{x}{\sigma_{wapp} \sqrt{2\pi t^3}} \exp\left(-\frac{(x - \mu_{wapp} t)^2}{2\sigma_{wapp}^2 t}\right), \quad t > 0 \quad (17)$$

where

$$\mu_{wapp} = V_0 - \frac{1}{2V_0} (k_y^2 \sigma_y^2 + k_h^2 \sigma_h^2), \quad \sigma_{wapp}^2 = \sigma_v^2 + \frac{1}{2V_0^2} (k_y^4 \sigma_y^4 + k_h^4 \sigma_h^4)$$

#### *Trajectory Uncertainty due to En-route Winds*

En-route wind uncertainties cause the aircraft ground speed to change, resulting in en-route service time variations. The ground speed of an aircraft  $V_g$  is given by

$$V_g = V_a + V_w \quad (18)$$

In the above equation,  $V_a$  is the air speed and  $V_w$  is the wind speed along track. The wind speed is a function of time and space. In the present research, the wind speed uncertainty is assumed to be a Gaussian random process, and its temporal variation in the body-fixed coordinates moving with the airplane is stationary and ergodic. By assuming that the mean value of the wind speed is piecewise constant over the flight path, the wind speed can be expressed as,

$$\begin{aligned} V_{w,i}(t, s_i) &= V_{w0,i}(t, s_i) + V'_{w,i}(t, s_i) \\ s_i &\in \{s_1, s_2, s_3 \dots, s_{n_s}\} \end{aligned} \quad (18)$$

where  $s_i$  is the spatially discretized  $i^{\text{th}}$  segment of the flight path,  $V_{w0}$  is the mean wind speed, and  $V_w'$  is the wind speed uncertainty. The wind speed in each segment can be represented as a white-Gaussian noise. That is,

$$V_{w,i} \sim N(V_{w0,i}, \sigma_{w,i}^2) \quad \text{or} \quad V'_{w,i} \sim N(0, \sigma_{w,i}^2) \quad (19)$$

With the airspeed being piecewise constant, the ground speed is also a Gaussian random variable.

$$V_{g,i} \sim N((V_{a,i} + V_{w0,i}), \sigma_{w,i}^2) \quad (20)$$

The corresponding service time uncertainty can be represented by the time integral of the reciprocal of Equation (21).

$$T = \int_s \frac{dt}{ds} ds = \int_s \frac{1}{s V_g} ds = \int_s \frac{1}{s (V_a + V_{w0} + V_w')} ds \quad (21)$$

The above equation can be evaluated in two different ways. The first approach is the computationally-intensive convolution of inverse Gaussian functions. The second approach is based on Gaussian approximation. The first will be briefly discussed here. Details on the second approach can be found in Reference 20.



The first step in this process is the approximation of variations in aircraft trajectory as Brownian motion with non-zero drift. The associated service time distribution in each flight path segment can be then be shown to follow the inverse Gaussian distribution<sup>24, 25</sup> or Wald's distribution:

$$f_s(t) = \frac{s}{\sigma_w \sqrt{2\pi t^3}} \exp\left(-\frac{(s - (V_a + V_{w0})t)^2}{2\sigma_w^2 t}\right), \quad t > 0 \quad (22)$$

Equation (22) represents the service time distribution for a single spatial segment. Several random variables with these inverse Gaussian distributions has to be convolved over all the flight segments to evaluate the service time distribution over a specified flight path. This convolution can be carried out over several representative paths in the airspace to create the overall wind uncertainty model.

*Trajectory Uncertainty due to Deviations Introduced by ATM*

The third en-route trajectory uncertainty considered in this paper is due to unplanned trajectory deviations commanded by the air traffic management system. These path changes are introduced primarily due to avoid severe weather, and sometimes due to traffic congestion, and introduce uncertainties in the en-route service time. These uncertainties are extracted from historic data by comparing *As-Filed* and *As-Flown* trajectories. The first represents the trajectory that the aircraft would have flown were it not for the ATM deviation, while the second represents the actual trajectory followed by the aircraft. The data for quantifying these uncertainties can be obtained from the FAA ASDI data feed. For the present study, the first occurrence of an aircraft flight plan in ASDI is assumed to be the As-Filed flight plan, and the subsequent occurrences are assumed to be As-Flown trajectory. A typical air traffic playback display in FACET using this logic is given in Figure 6. The solid blue line represents the As-Filed flight plan and the dotted red line represents the trajectory reported by aircraft. Comparisons in the flight durations between such pairs of trajectories provide the desired data. The derived statistics is then used to evaluate the service time uncertainty for use with the queuing network analysis.

Figure 7 shows the distributions of the nondimensional time (ratio of the as-flown time and the as-filed time) calculated from the actual ASDI data for August 24, 2005. The mean values are very close to 1, and the distributions are slightly right-skewed, i.e. the right tail is longer. It means that, on an average, the actual duration of flight is close to the expected duration, and the time distribution of delay is more uncertain and spread than the distribution of earlier-than-scheduled flights. Statistical values for two different dates are present in Table 3.

**Table 3. Statistical Properties of the ATM-introduced Service Time Distributions**

	Date	
	July 13, 2005	August 24, 2005
Mean	1.0147	1.0207
Standard Deviation	0.0948	0.0978
Skewness	0.7985	0.8783

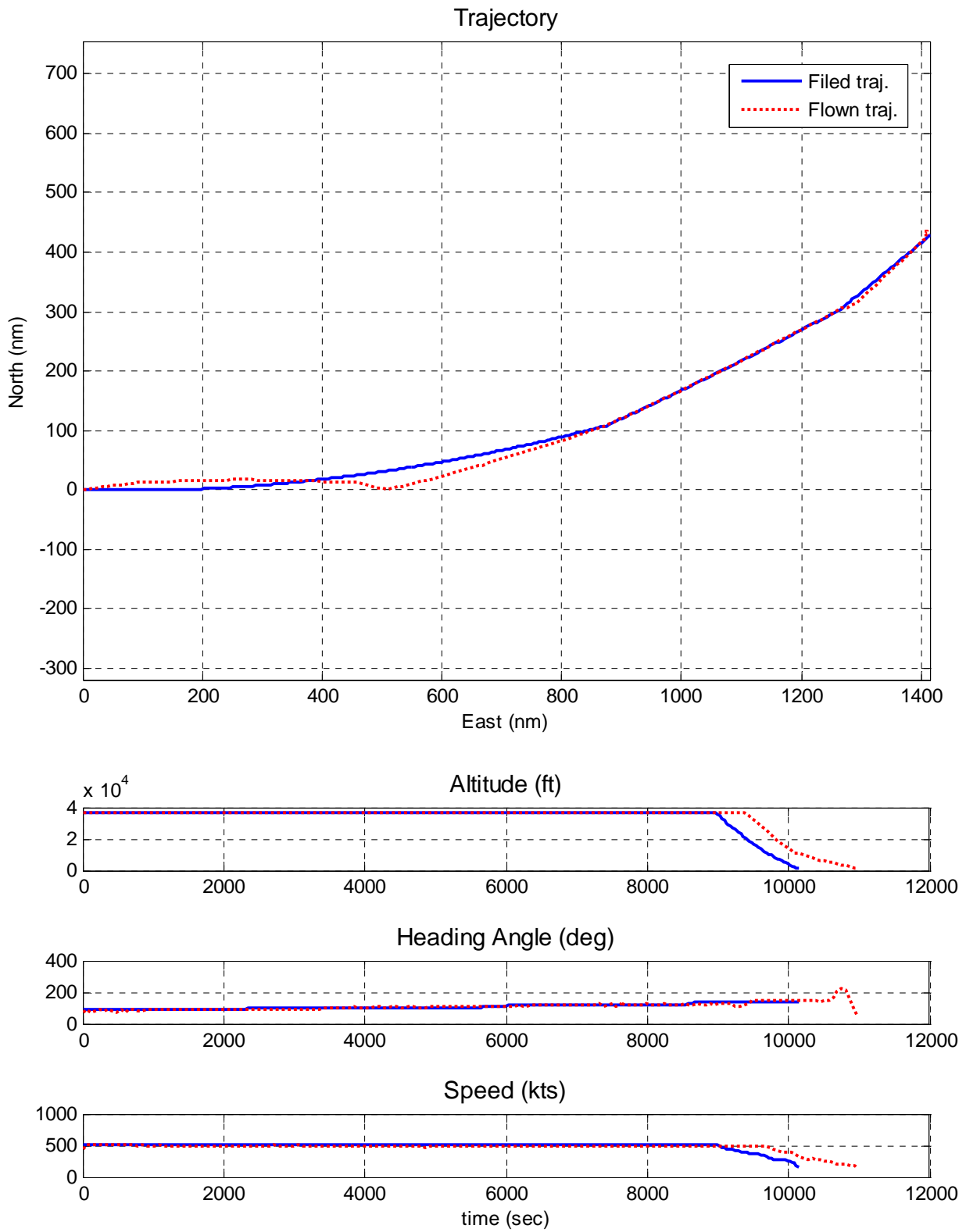
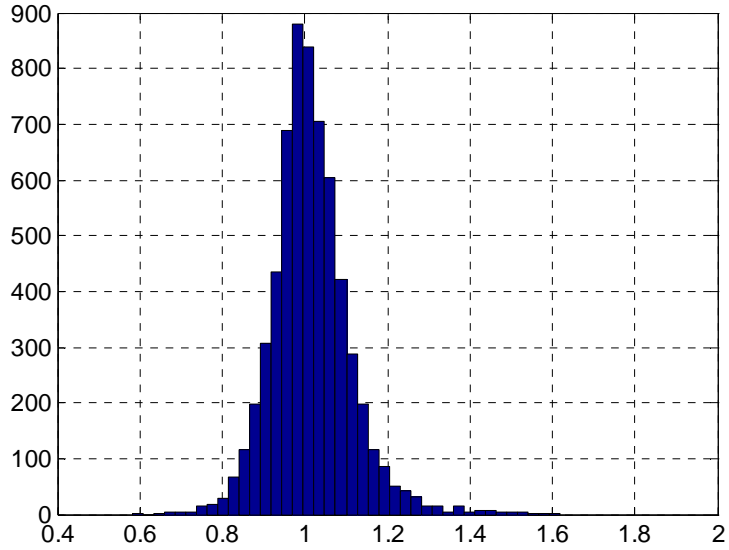
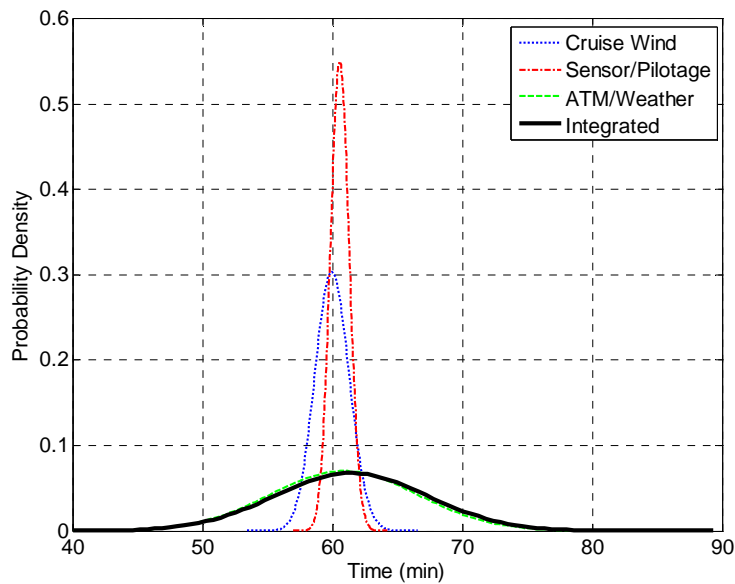


Figure 6. A typical *As-Filed* (Blue) and *As-Flown* (Dotted Red) Trajectories



**Figure 7. Normalized Service Time Distribution due to ATM Deviations on August 24, 2005 (As-Flown vs. As-Filed)**

The uncertainties introduced by navigation and control, cruise wind and ATM discussed in the foregoing sections can be convolved to generate the overall service time uncertainty distributions. Figure 8 shows the service time distribution due to the integrated en-route uncertainties. These service time distributions can then be used in the queuing networks to assess their impact of the traffic flow metrics as will be illustrated in the following section.



**Figure 8. Integrated En-Route Service Time Distribution (with Autopilot, Nominal Flight Time = 1 hour)**

### III. Air Traffic Flow Analysis using Queuing Network Models

The traffic flow parameters computed using the approaches outlined in the foregoing section is used to formulate queuing network models of the NAS. As stated at the beginning of this paper, two distinct types of queuing networks were employed in the present research. The first is the open Jackson or Markovian queuing network<sup>4</sup>, and the second is a refinement of the first through the use of the QNA approximation<sup>6</sup>. The chief difference between the

two is that in the case of Markovian queues, a single parameter, namely, the mean or the variance defines each of the stochastic distributions in the queuing networks. If this definition is acceptable, Jackson queuing networks provide exact algebraic expressions for describing the queuing phenomena. On the other hand, the QNA approximation allows the definition of a distinct mean and a variance for each of the distributions in the network. However, the queuing results are only approximate. Using Monte Carlo simulations, the present research has verified that the QNA approximation provides excellent approximation to the queuing phenomena in the NAS. The following section will first present an analysis of the NAS using the Jackson network formulation. A more detailed discussion of the Jackson queuing networks of the NAS can be found in Reference 26. This will be followed by a section discussing the QNA approximation of the queuing networks.

#### A. Analysis of the NAS using Open Jackson Queuing Networks

A Jackson Network can be characterized as a network of  $N$  service nodes where each service node  $j$  ( $j = 1..N$ ) has an infinite waiting space in the queue.

1. Customers arrive from outside the system according to a Poisson input process (Exponential inter-arrival times) with mean arrival rate  $p_{0j}$ .
2. Each node has  $m_j$  parallel servers with exponential service time distribution with mean service rate  $\mu_j$ .
3. A customer leaving node  $i$  is routed to an adjacent node  $j$  with flow fraction  $q_{ij}$  or departs the system with probability  $1 - \sum_{j=1}^n q_{ij}$ . The inter-arrival time distributions, service time distributions and flow fractions from FACET runs can be used to construct Airspace-level, Center-level, Sector-level and latitude/longitude-level Open Jackson queuing networks.

It has been demonstrated that under steady state conditions, each node  $j$  in the Jackson network behaves as if it were an independent  $M / M / m_j$  queuing system with arrival rate  $\lambda_j$  obeying the flow-balance equation

$$\lambda_j = p_{0j} + \sum_{i=1}^n \lambda_i q_{ij} \quad (23)$$

where  $m_j \mu_j > \lambda_j$  will ensure that the steady-state can be attained. Since each node behaves as an independent queuing system, it can be analyzed separately. This fact allows the separate treatment of each node, with the flow balance requirement tying the back solutions together. The matrix form of the flow-balance equations is:

$$\boldsymbol{\lambda} = (\mathbf{I} - \mathbf{Q}^T)^{-1} \mathbf{p}_0 \quad (24)$$

After calculating the arrival rates  $\boldsymbol{\lambda}$ , each node is analyzed independently as follows. Let  $P_{nj}$  indicate the probability that  $n$  customers are present at node  $j$ . The quantities  $P_{0j}$  and  $P_{nj}$  are calculated as:

$$P_{0j} = \frac{1}{\sum_{i=0}^{m_j-1} \frac{(\lambda_j / \mu_j)^i}{i!} + \frac{(\lambda_j / \mu_j)^{m_j}}{m_j!} \frac{1}{1 - \lambda_j / (m_j \mu_j)}} \quad (25)$$

$$P_{nj} = \begin{cases} \frac{(\lambda_j / \mu_j)^n}{n!} P_{0j} & \text{if } 0 \leq n < m_j \\ \frac{(\lambda_j / \mu_j)^n}{m_j! m_j^{(n-m_j)}} P_{0j} & \text{if } n \geq m_j \end{cases} \quad (26)$$

Expected queue length at node  $j$  (excluding customers being served) is calculated as

$$L_{qj} = \frac{P_{0j} (\lambda_j / \mu_j)^{m_j} \rho_j}{m_j! (1 - \rho_j)^2} \quad (27)$$

where  $\rho_j = \lambda_j / (m_j \mu_j)$ . The expected queue length at the nodes indicates the number of aircraft in that are subjected to delays due to air traffic congestion. Expected number of customers at the node being served and waiting, is given by

$$L_j = L_{qj} + \frac{\lambda_j}{\mu_j} \quad (28)$$

Expected waiting time in the queue, excluding the time while being served is

$$W_{qj} = \frac{L_{qj}}{\lambda_j} \quad (29)$$

The expected waiting time in the queue indicates the average delay experienced by the aircraft due to congestion. Expected system time including both waiting and service times is given by:

$$W_j = W_{qj} + \frac{1}{\mu_j} \quad (30)$$

The expected system time indicates the total flight time through a Center including the delays due to congestion.

The quantities calculated in the foregoing can be used to quantify the traffic flow efficiency through a given node as

$$\text{Traffic Flow Efficiency} = \frac{E(\text{System Time}) - E(\text{Wait Time})}{E(\text{System Time})} \quad \text{i.e.} \quad E_j = \frac{E(W_j) - E(W_{qj})}{E(W_j)} \quad (31)$$

where  $E(.)$  denotes the expected value. The traffic flow efficiency along a path in the airspace can be obtained as

$$E_{\text{path}} = \frac{\sum_{j=1}^n \{E(W_j) - E(W_{qj})\}}{\sum_{j=1}^n E(W_j)} \quad (32)$$

where  $j = 1..n$  denotes all the nodes traversed along the path.

As an example of the type of results that can be derived from the Jackson queuing networks of the NAS, the following figures illustrate the national traffic flow characteristics at Sector-level spatial resolution. Some of the traffic flow metrics referenced in these figures are from Reference 27. Figure 10 through Figure 16 show the traffic intensities, mean delay and path efficiency from KLAX to other major airports in the NAS.

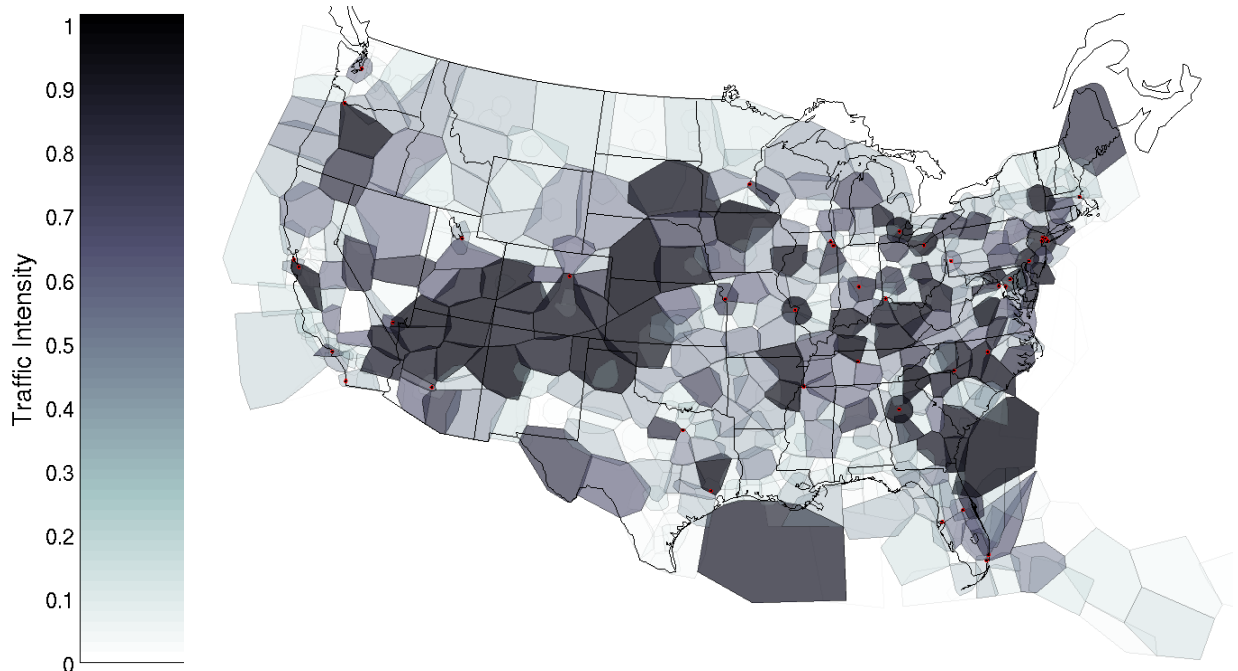


**Figure 9. Traffic Intensity at Various Sectors in the NAS**

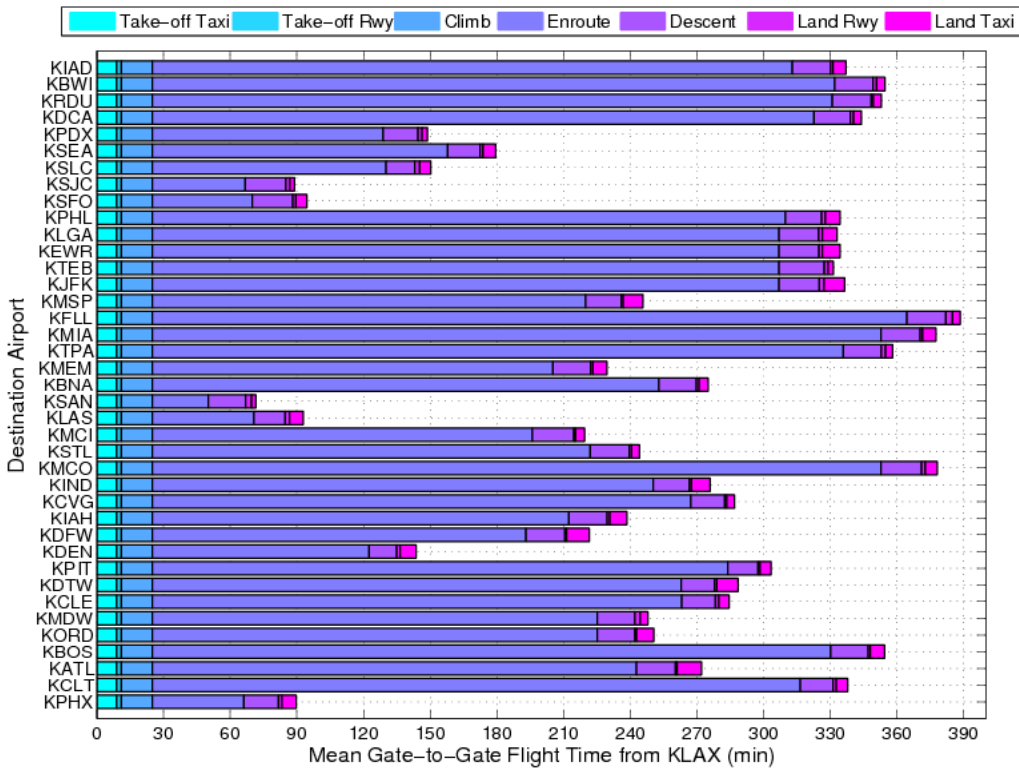


Figure 10. Mean Gate-to-Gate System Times using Markovian Analysis with Nominal Data

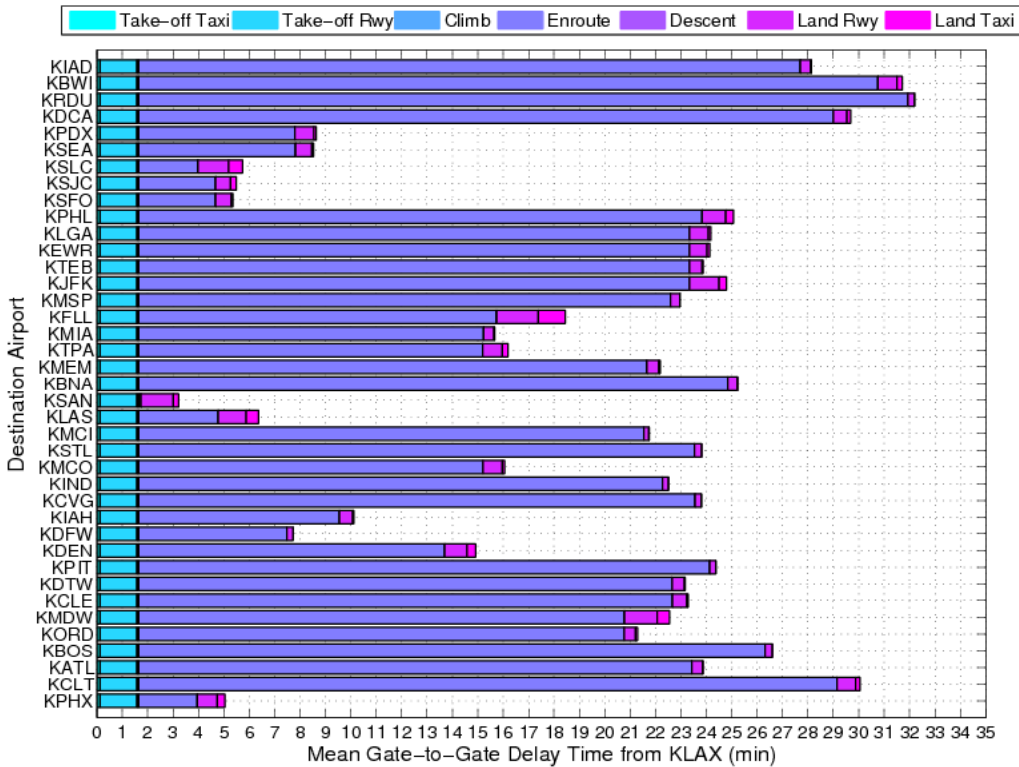


Figure 11. Mean Gate-to-Gate Delays using Markovian Analysis with Nominal Data

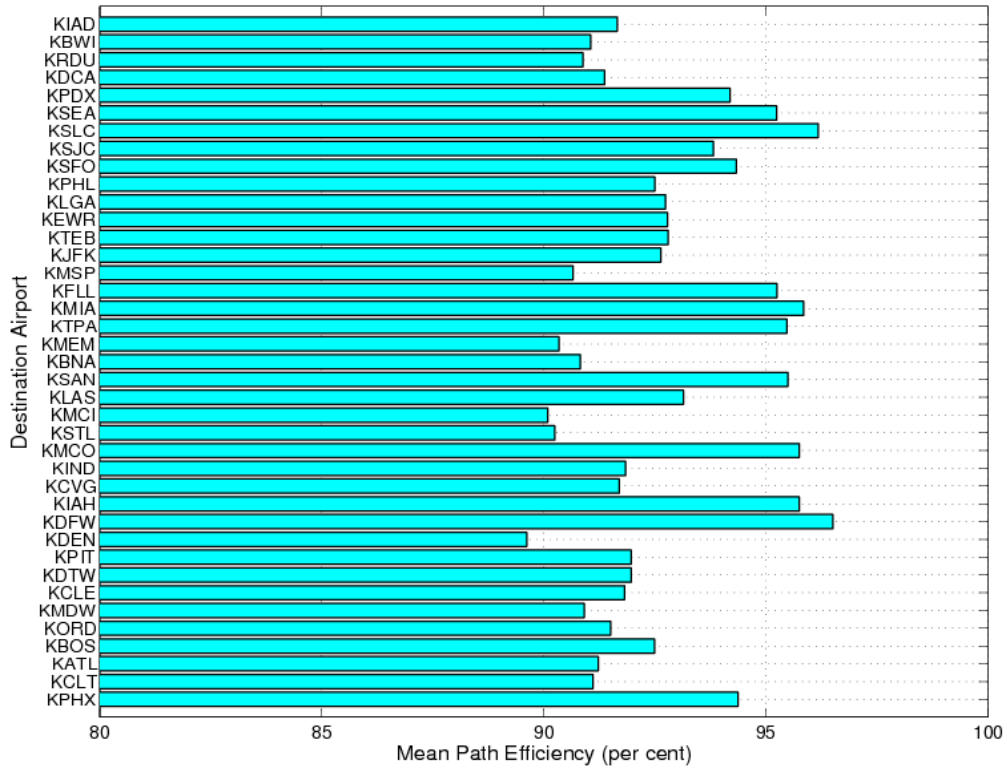


Figure 12. Mean Gate-to-Gate Efficiencies using Markovian Analysis with Nominal Data

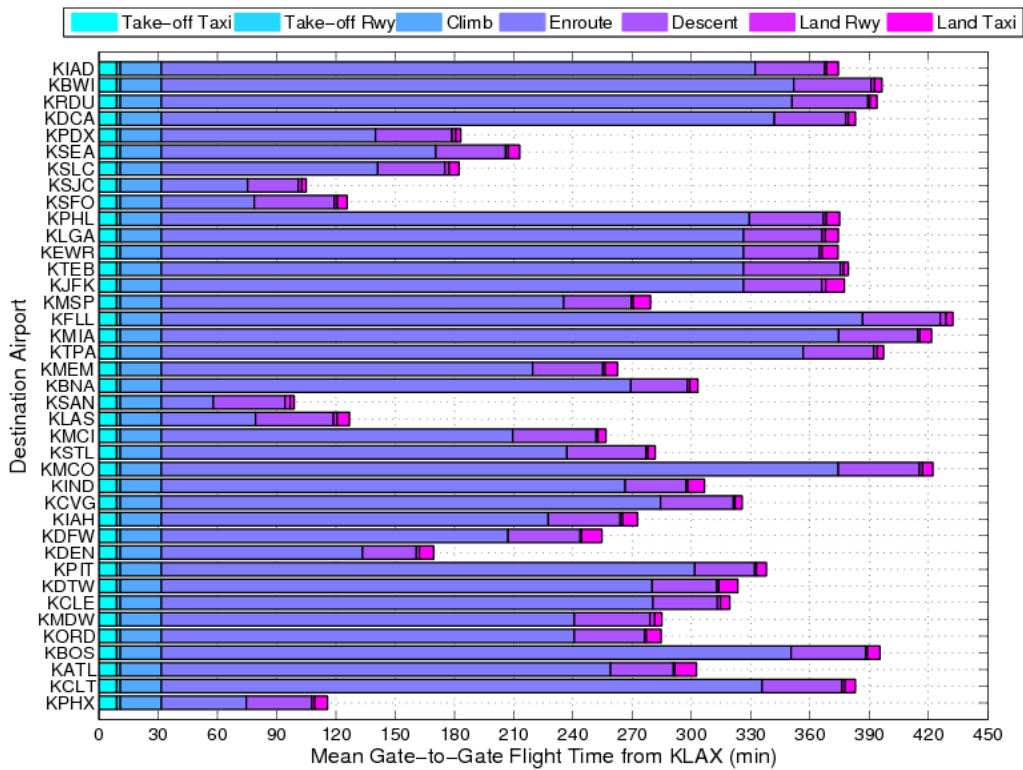


Figure 13. Mean Gate-to-Gate System Time using Markovian Analysis with Uncertainties

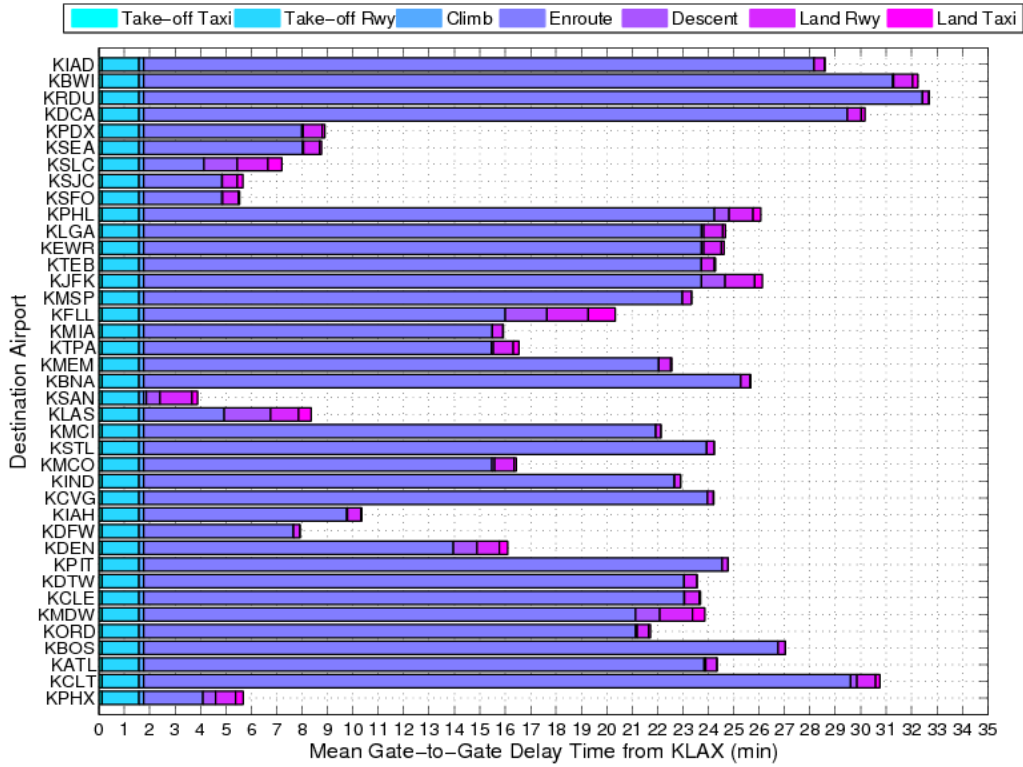


Figure 14. Mean Gate-to-Gate Delay Time using Markovian Analysis with Uncertainties

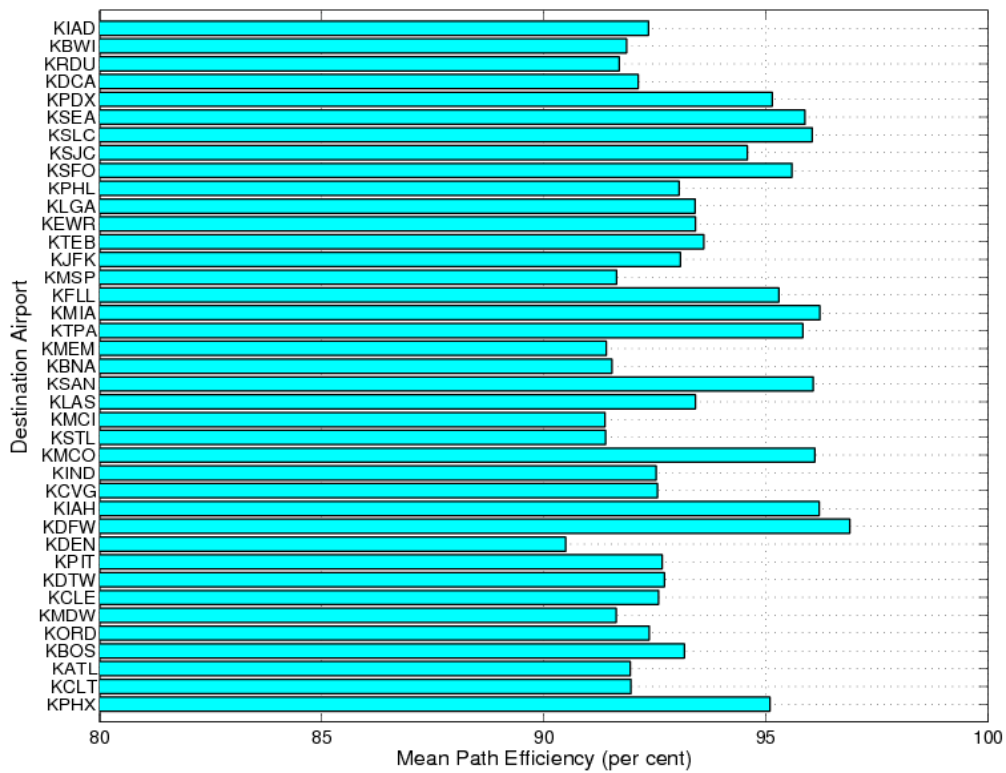
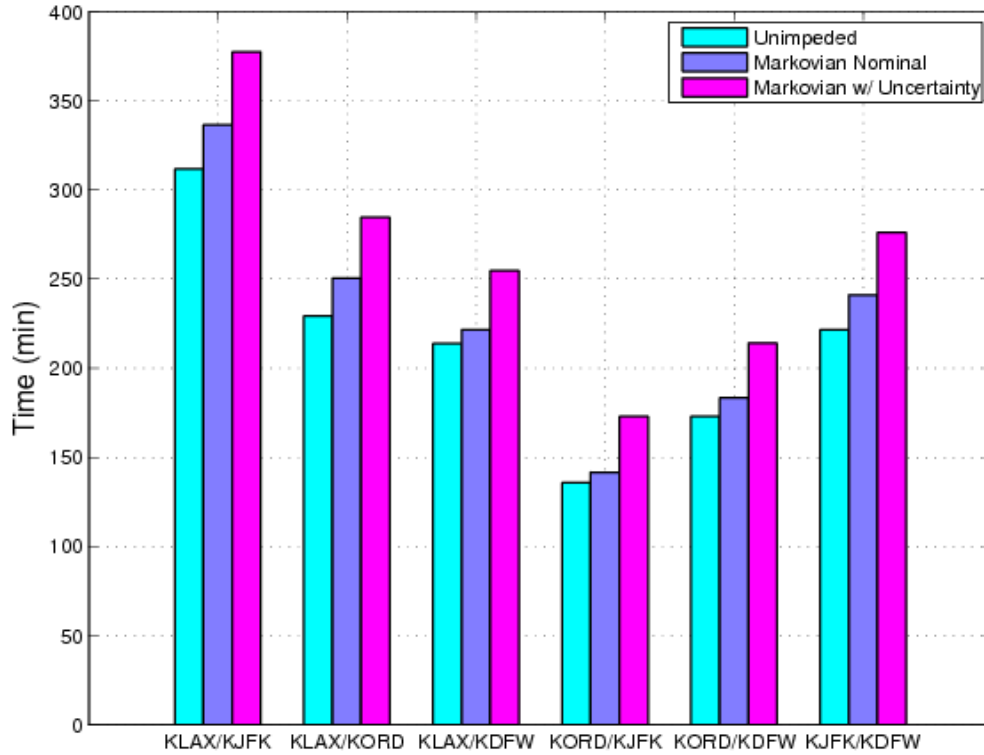


Figure 15. Mean Gate-to-Gate Efficiencies using Markovian Analysis with Uncertainties





**Figure 16. Comparison of Total Gate-to-Gate Times Using Markovian Analysis**

Once the inter-arrival rate distributions, service time distributions and the flow fractions are specified, the data given in these figures can be generated in under one second. This makes the queuing analysis valuable in conducting trade studies of various types. These models can also be valuable for real time traffic flow management decision making.

### B. Analysis of the NAS using QNA Approximation

The Queuing Network Analyzer<sup>6</sup> (QNA) approximation builds on the well-known Markovian model for M/M/s (Markovian arrival, Markovian service process with s parallel servers). As noted at the beginning of this section, in a Markovian queuing model, the mean cannot be differentiated from the variance and only Markovian inputs are allowed for the arrival and service distributions. On the other hand, the QNA model permits the specification of first and second moments of arbitrary arrival and service distributions, which may better approximate the real processes. Note that while Markovian analysis is an exact solution to an approximate model that only fits the inter-arrival and service time distribution mean values, the QNA is an approximate solution to a higher-fidelity model that matches the inter-arrival and service time distributions more closely.

As in the Markovian networks, the mean traffic flows into queuing network nodes (i.e. the internal arrival rates) are estimated by solving the flow balance equations. The expected flow rate through each node ( $\lambda_i$ ) is given by

$$\lambda_j = p_{0j} + \sum_{i=1}^n \lambda_i q_{ij} \quad (33)$$

where  $n$  is the number of nodes,  $q_{ij}$  is the fraction of customers in the  $i$ th node that go to the  $j$ th node upon completing service, and  $p_{0j}$  is the external arrival flow rate at the  $j$ th node.

The QNA model builds on the flow balance calculation by introducing the variances for these internal arrival rates. The heart of the QNA approximation is the system of equations yielding the variability parameters for the internal flows, i.e., the squared coefficients of variation, defined as the ratio of the variance of the distribution and the squared mean. The coefficient of variation of the arrival distribution at the  $j$ th node,  $c_{a_j}^2$ , are given by the following expression:

$$c_{a_j}^2 = a_j + \sum_{i=1}^n c_{a_i}^2 b_{ij} \quad (34)$$

where  $a_j$  and  $b_{ij}$  are constants depending on the input data:

$$\begin{aligned} a_j &= 1 + w_j \left\{ (p_{0j} c_{0j}^2 + 1) + \sum_{i=1}^n p_{ij} [(1 - q_{ij}) + (1 - v_{ij}) \gamma_i q_{ij} \rho_i^2 x_i] \right\} \\ b_{ij} &= w_j p_{ij} q_{ij} \gamma_i [v_{ij} + (1 - v_{ij})(1 - \rho_i^2)] \end{aligned} \quad (35)$$

In this equation, the variables  $x_i$ ,  $v_{ij}$ , and  $w_{ij}$ , are dependent on the utilization factor at the  $i$ th node,  $\rho_i$ , the number of servers at the  $i$ th node,  $m_i$ , and the squared coefficient of variation of the service time at the  $i$ th node,  $c_{s_i}^2$ . In the version of the QNA algorithm used here, formulae for these variables are obtained as<sup>6</sup>:

$$\begin{aligned} x_i &= 1 + \sqrt{\frac{1}{m_i} (\max\{c_{s_i}^2, 0.2\} - 1)} \\ v_{ij} &= 0 \\ w_j &= [1 + 4(1 - \rho_j)^2 (v_j - 1)]^{-1} \\ v_j &= \left[ \sum_{i=0}^n p_{ij}^2 \right]^{-1} \end{aligned} \quad (36)$$

The variable  $p_{ij}$  is obtained from the formula  $p_{ij} = \lambda_{ij}/\lambda_j$  where  $\lambda_{ij} = \lambda_i q_{ij}$  is the mean flow rate from the  $i$ th node to the  $j$ th node. The key approximations, given by Equations (35) and (36), which yield the variability parameters for the internal flows are all based on the basic method discussed in Reference 6, viz. asymptotic methods and the stationary interval method. Using the theory in Reference 6, the squared coefficients of variation of a split process (for example, flows from one node to several other nodes) is given by:

$$c_i^2 = p_i c^2 + 1 - p_i, \quad i = 1, 2, \dots, k \quad (37)$$

where  $p_i$  is the flow fraction into the  $i$ th node. For example, the squared coefficient of variation of flows departing the network at the  $i$ th node is given by Equation (37) with  $p_i = (1 - \sum_{j=1}^n q_{ij})$ .

For the departure process from a node, Reference 6 uses the following formula for the squared coefficient of variation of inter-departure time:

$$c_d^2 = 1 + (1 - \rho^2)(c_a^2 - 1) + \frac{\rho^2}{\sqrt{m}}(c_s^2 - 1) \quad (38)$$

After completing the variance propagation throughout the network, the first two moments for the arrival process into each node are available and hence each node can be analyzed in isolation. The M/M/s queuing model is applied to each node to determine the nodal queuing metrics such as the number of aircraft in the system  $L$ , the number in the queue  $L_q$ , the total average time spent by an aircraft in the system  $W$ , and the time spent in the queue  $W_q$ . The nodal queuing metrics are calculated using the following QNA approximations for the general arrival process, general service processes and multiple-server queues (G/G/s):

$$W_{qQNA} = \left( \frac{c_a^2 + c_s^2}{2} \right) W_{qJackson} \quad (39)$$

where  $W_{q_{QNA}}$  and  $W_{q_{jackson}}$  are the waiting time in queue for the QNA algorithm and Jackson Network solution, respectively, and  $c_a^2$  and  $c_s^2$  are the squared coefficients of variation of the inter-arrival time and service time of a node. Based on Equation (39) and Little's Formula

<sup>19</sup>, the number of items in queue is found by the formula  $L_{q_{QNA}} = \lambda W_{q_{QNA}}$ . The mean time in service and mean number in service are found by the formulae  $W_{QNA} = W_{q_{QNA}} + 1/\mu$ , and  $L_{QNA} = \lambda W_{QNA} = L_{q_{QNA}} + \lambda \rho m$ , respectively. The variance of these four queuing parameters are assumed to be the same regardless of whether the Jackson Network solution is used, or whether the QNA algorithm is used.

The QNA approximation is next used to derive traffic flow results for Sector-level spatial discretization of the NAS. The results given in Figure 17 through Figure 23 given this subsection parallels those in the previous section on Markovian Sector-level queuing network. Note that the results are similar, but not identical. It is expected that the QNA approximation will yield better results than the Markovian model, since the real distributions of inter-arrival and service times contain distinct first and second moments. This fact will be demonstrated in the next section through Monte Carlo simulations.

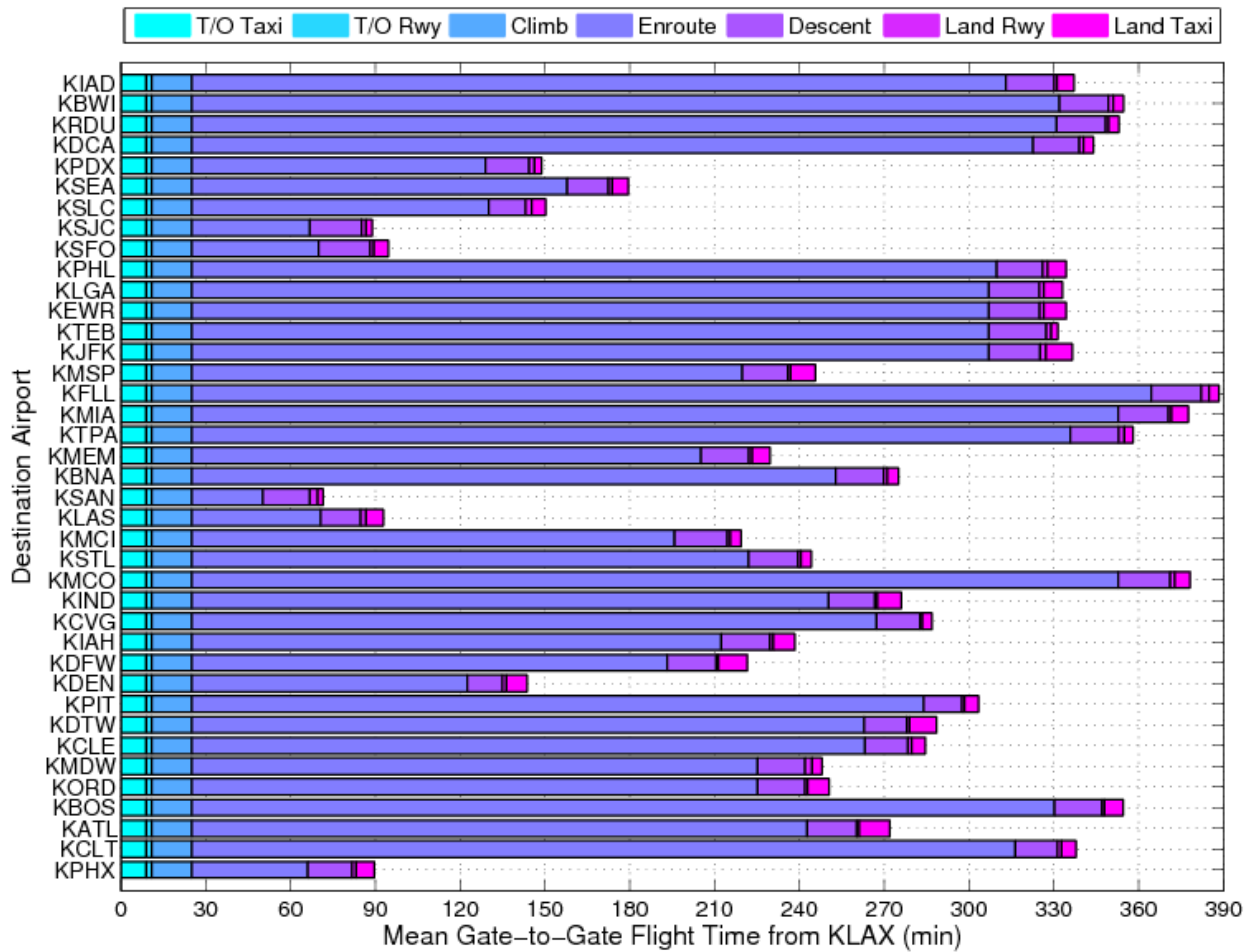


Figure 17. Mean Gate-to-Gate System Times using QNA Analysis with Nominal Data

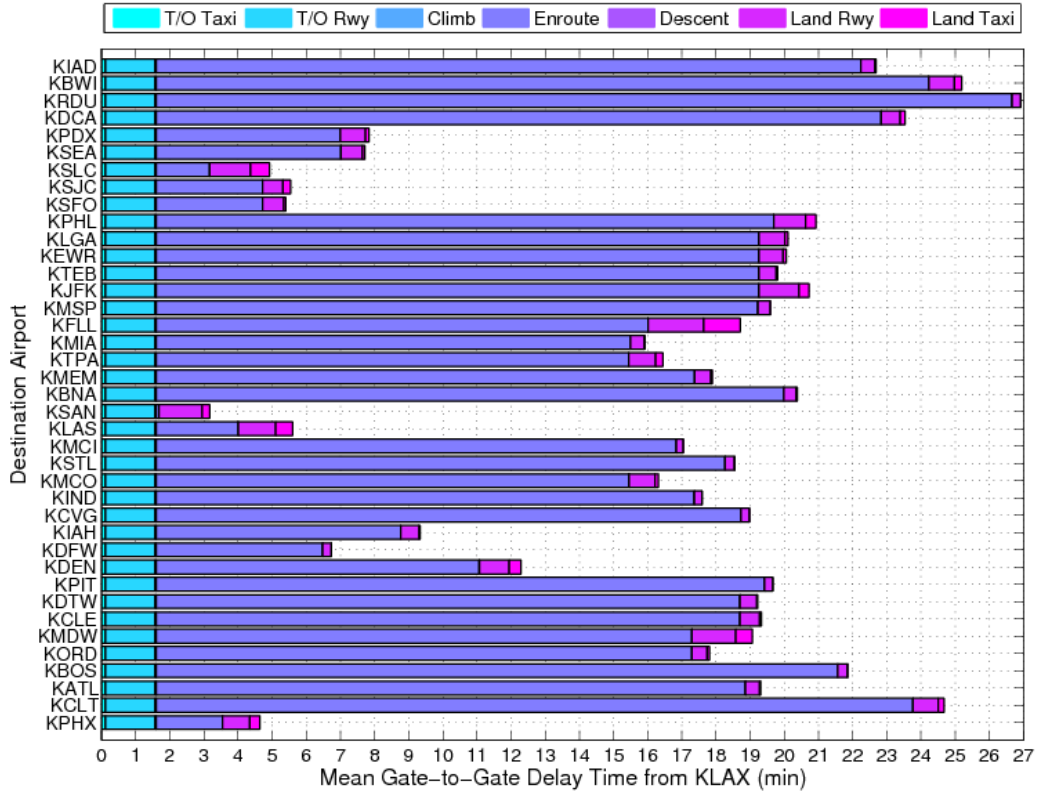


Figure 18. Mean Gate-to-Gate Delays using QNA Analysis with Nominal Data

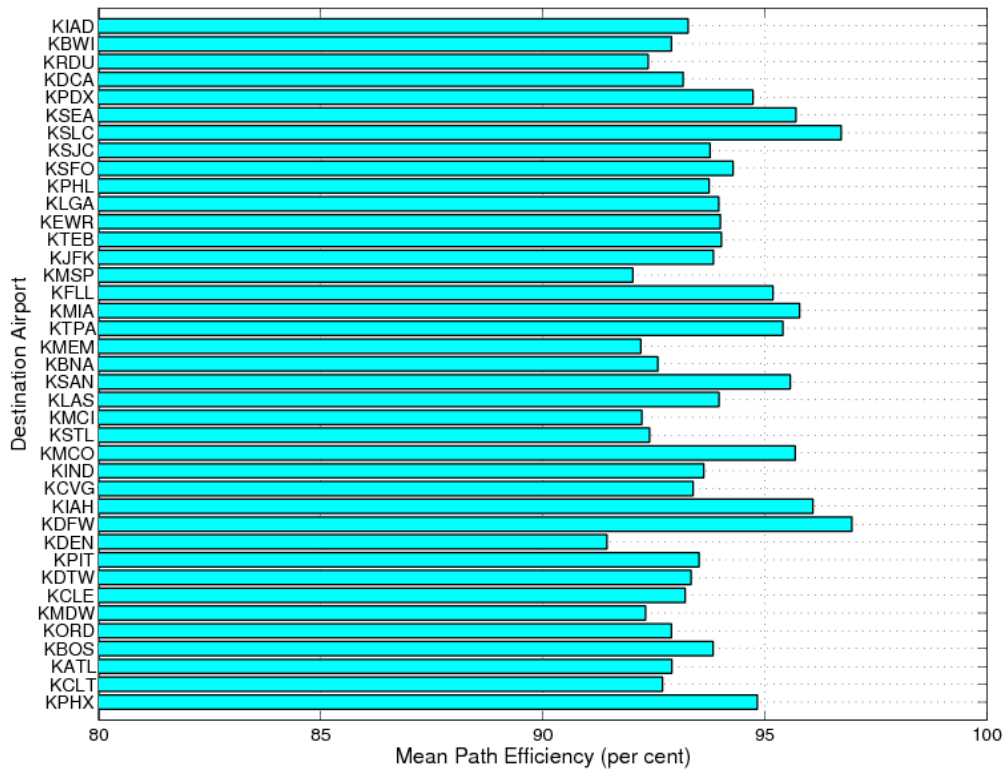


Figure 19. Mean Gate-to-Gate Efficiencies using QNA Analysis with Nominal Data

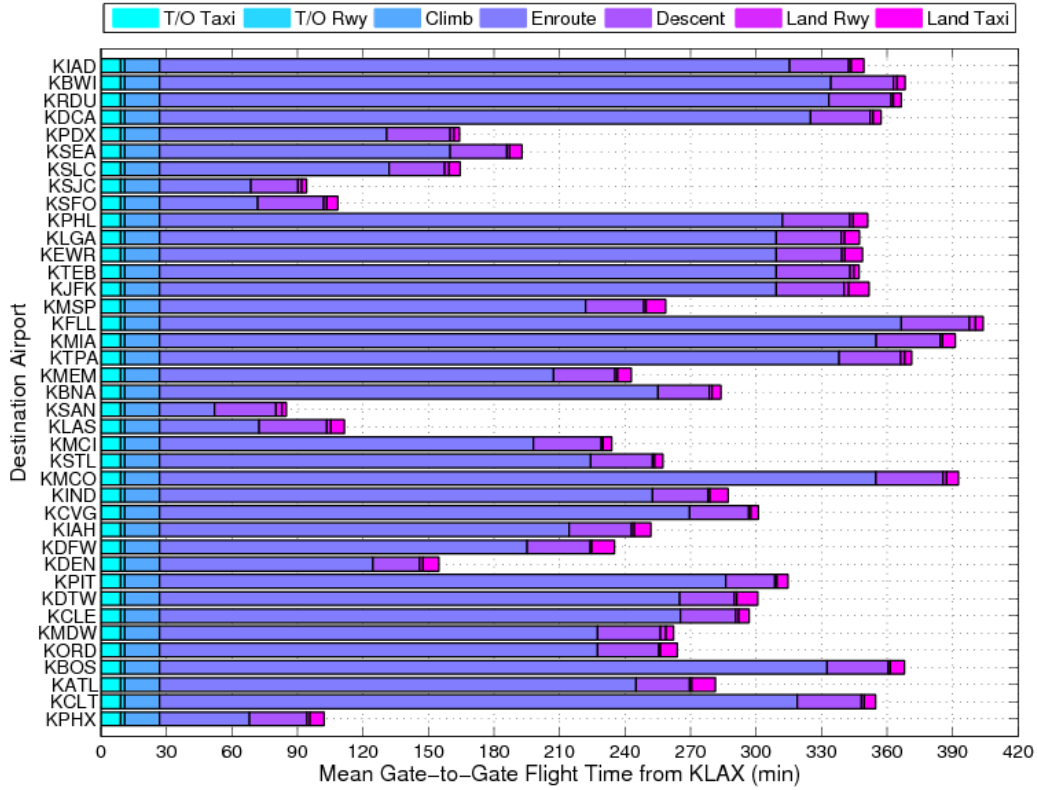


Figure 20. Mean Gate-to-Gate System Times using QNA Analysis with Uncertainties

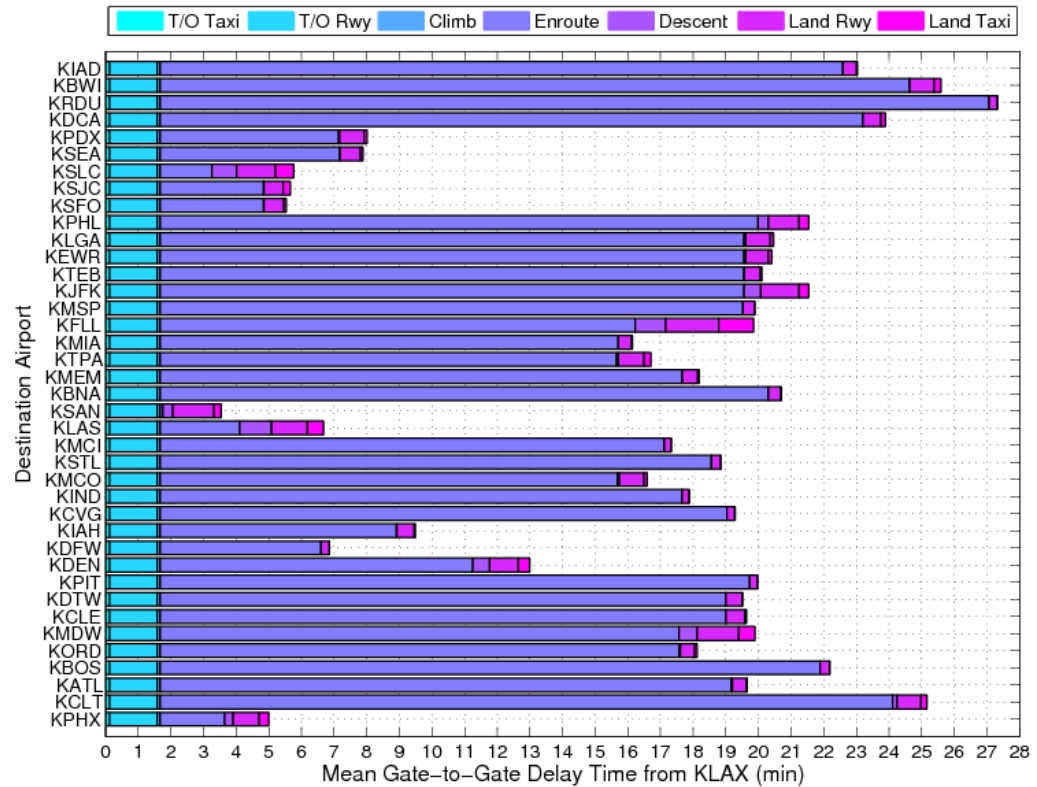


Figure 21. Mean Gate-to-Gate Delays using QNA Analysis with Uncertainties

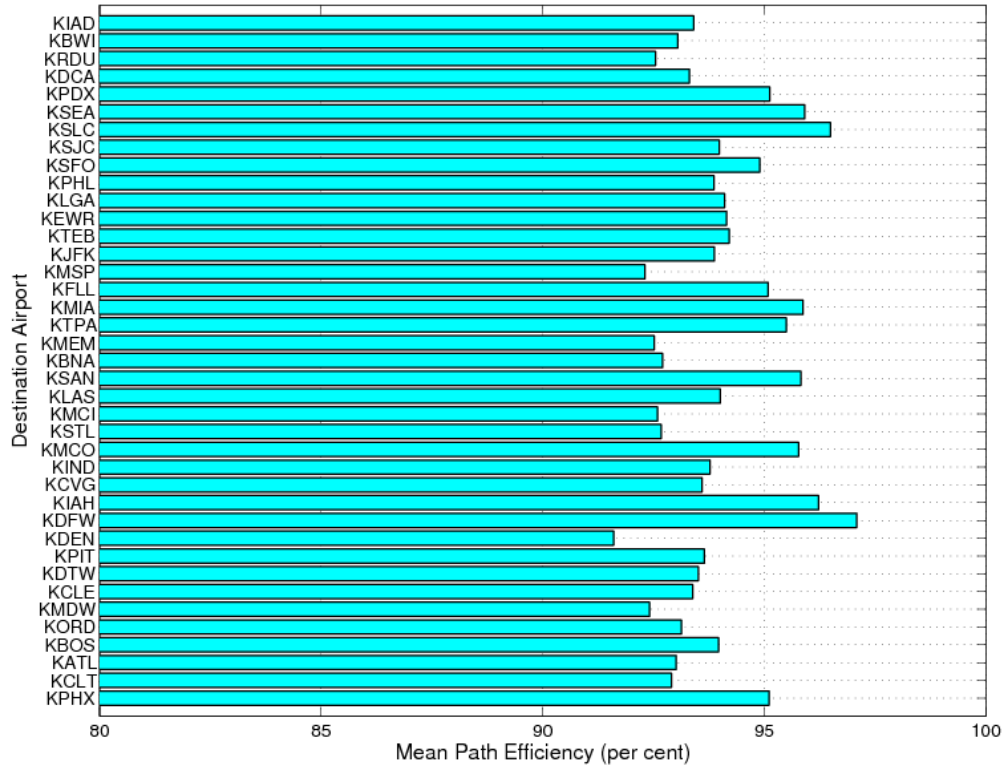


Figure 22. Mean Gate-to-Gate Efficiencies using QNA Analysis with Uncertainties

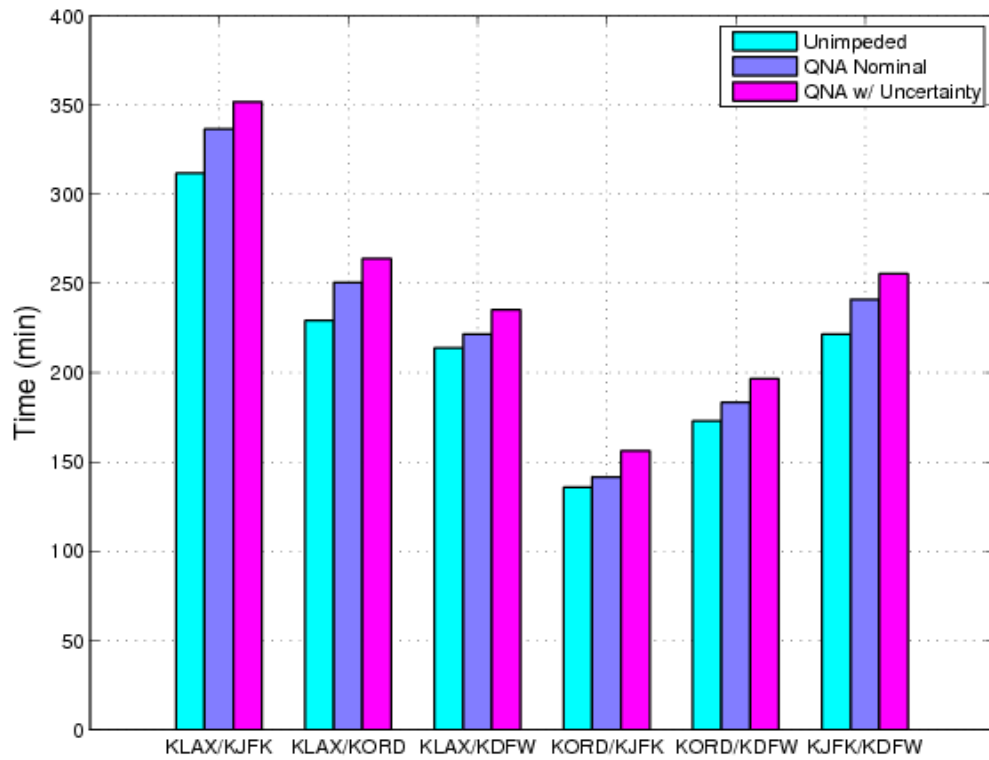


Figure 23. Comparison of Total Gate-to-Gate Times Using QNA Algorithm

### III. Comparison between Queuing Networks and Monte Carlo Simulations

Monte Carlo simulation is a general approach for evaluating the stochastic characteristics of arbitrary nonlinear dynamical systems involving non-Gaussian distributions. Since the distributions used in the queuing networks are derived from historic data, they are far different from the ideal Markovian distributions. Consequently, the computation of the traffic metrics using Markovian and QNA approximation-based queuing networks are likely to be inaccurate. Hence, Monte Carlo simulations must be employed to assess the fidelity of the queuing network models. Validation of the queuing network at Center-level discretization of the NAS will be discussed in this section. The data used in the present study is derived from one-day ASDI traffic data feed, by eliminating duplicate flights. This step is essential to remove the effects of trajectory deviations due air traffic management (ATM) actions and adverse weather. As discussed elsewhere in this paper, both of these are separately modeled as trajectory uncertainties in the present formulation. The following will present comparisons between the Monte Carlo simulation, Center-level Jackson and QNA network, and FACET simulations.

Monte Carlo simulation of the queuing network is set up with specified inter-arrival and service time distributions, together with traffic flow fractions at each node. As a first step of validation process, Monte Carlo simulations are carried out to verify that it can reproduce the analytical results from Jackson network model of the NAS. In this model, FACET simulations are used to obtain service rates and external arrival rates from airports. These rates are used to generate random numbers from corresponding exponential deviates. Using 50000 samples per airport, flow rates through all nodes in the network can be calculated. This process demonstrated that the Monte Carlo simulations are able to recreate Jackson network results with a high degree of accuracy.

Monte Carlo simulation are next conducted with 200,000 samples inserted at the airport taxi arrival point. This results in  $200,000 \times 180 = 900,000,000$  total samples in the network. On a quad-core 64-bit processor at 2.6GHz, the simulations consumed 44 hours. The Monte Carlo simulations do not assume any particular form for the service time or inter-arrival time distributions, but instead sample points from the histograms of data derived from FACET runs, using the rejection method<sup>24</sup> of sampling.

The network solution can provide flow metrics and queuing parameters at all nodes. Figure 24 and Figure 25 provide comparisons of the mean and standard deviation of inter-arrival and inter-departure time for flows entering and leaving the Center node from Monte Carlo simulations and the QNA network. The mean flow rate in the QNA model is obtained from a Jackson network solution, and as a consequence, the mean inter-arrival time and mean inter-departure time for a node are identical for these networks. As can be observed from Figure 24, the mean values from Monte Carlo and QNA network are nearly-identical; with the error being less than 0.01% in all nodes.

The standard deviations of the inter-arrival and inter-departure time distributions for a node are not necessarily the same, even though the mean values are the same. The standard deviation of the inter-departure time compared with the value predicted by QNA approximation, is shown in Figure 25. While the values from Monte Carlo simulations and the QNA solution are not identical, QNA provides a good representation of the standard deviation values of the interval time of the departing items. It is implicitly assumed here that the standard deviation values from Monte Carlo simulations are more accurate than those of the QNA model because they use histogram information rather than an assumed form of service time and arrival time probability density functions (PDFs). Furthermore, the QNA model is known to be an approximate solution.

Figure 26 compares the mean number of aircraft in the Centers at any given time between the QNA model and FACET simulations, and with Monte Carlo simulations. It can be observed that the values obtained from QNA, Monte Carlo simulations and FACET simulations are in close agreement. The QNA model uses Jackson network results for the mean number of items in the system, with modifications introduced to account for the second moment of the arrival and service processes. The mean number in the system from Monte Carlo simulations is obtained from a histogram of the counts in the node, based on the time of arrival or departure of a sample. FACET simulations can be used to obtain the number of aircraft in a Center at any given time; the time-average over a 24 hr period is used to calculate the FACET mean.

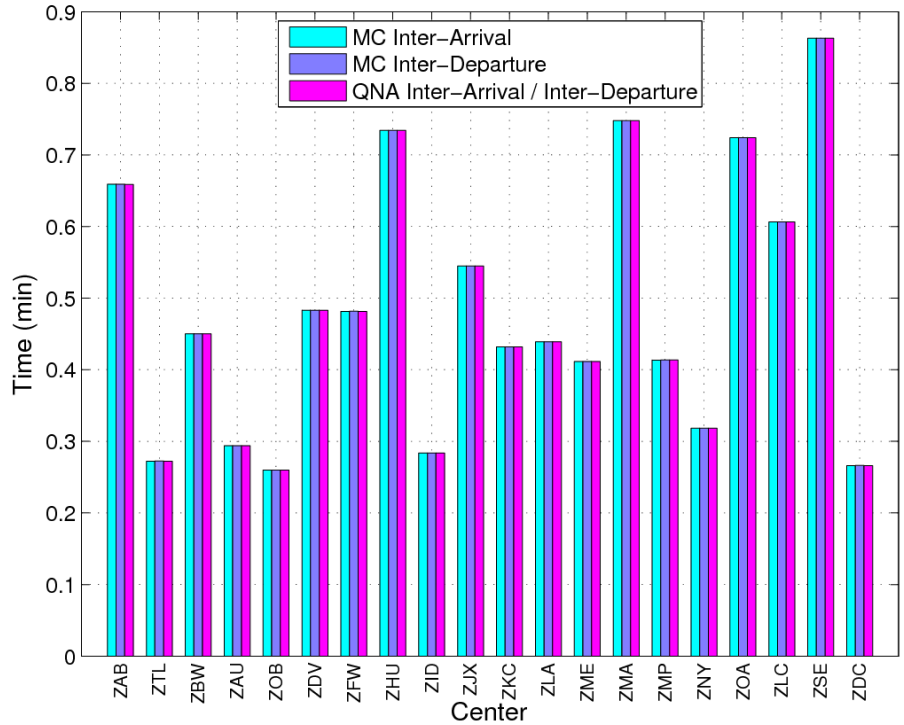


Figure 24. Mean Inter-Arrival and Inter-Departure Times of Aircraft from Centers

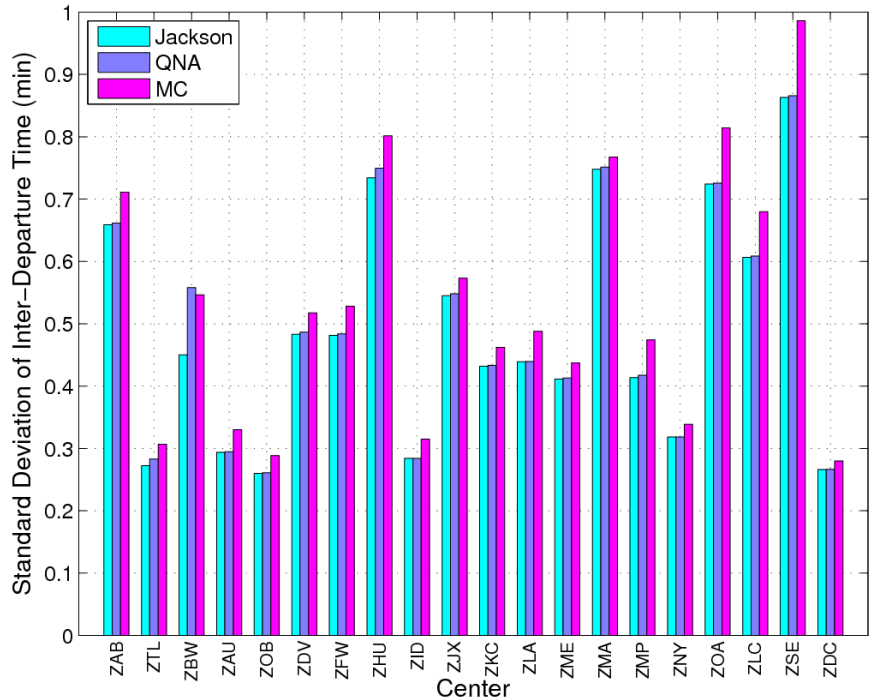


Figure 25. Standard Deviation of Inter-Departure Times of Aircraft from Centers



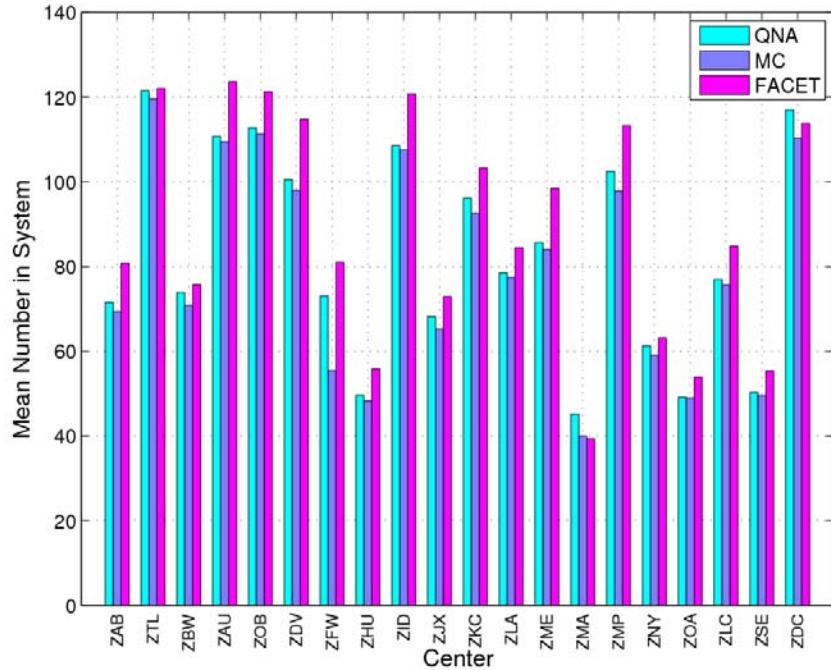


Figure 26. Mean Aircraft Count in Centers

The results from the QNA approximation diverge further from Monte Carlo simulations when the standard deviations of the number of aircraft in the Centers from both approaches are compared. These are shown in Figure 27, compared alongside with the results obtained from FACET. Standard deviation from FACET data is found to differ by more than 100% of the nominal MC standard deviation. This can be attributed to size of samples from which standard deviation is calculated for each Center. It is expected that at finer spatial resolutions, more favorable comparisons may be achievable for the standard deviations.

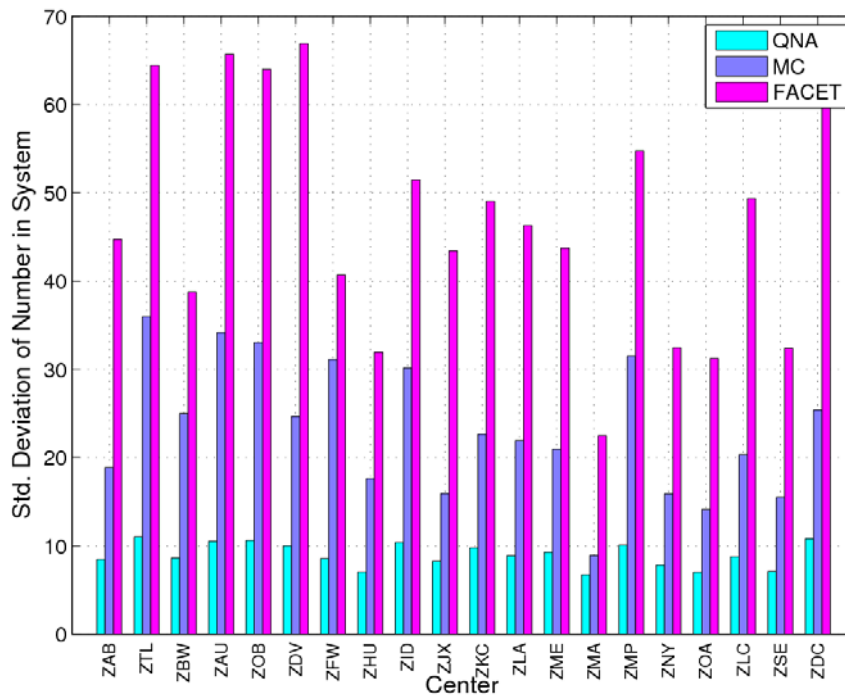


Figure 27. Standard Deviation of Aircraft Count in Centers

The flow rates derived from the QNA queuing network is next compared with those from the Monte Carlo simulation and FACET. The mean values from the Monte Carlo simulation, Center-level QNA network and FACET are presented in Figure 28. This figure shows that Monte Carlo simulations agree very well with QNA results, with the error being less than 0.01% of the nominal mean inter-arrival time from Monte Carlo simulations.

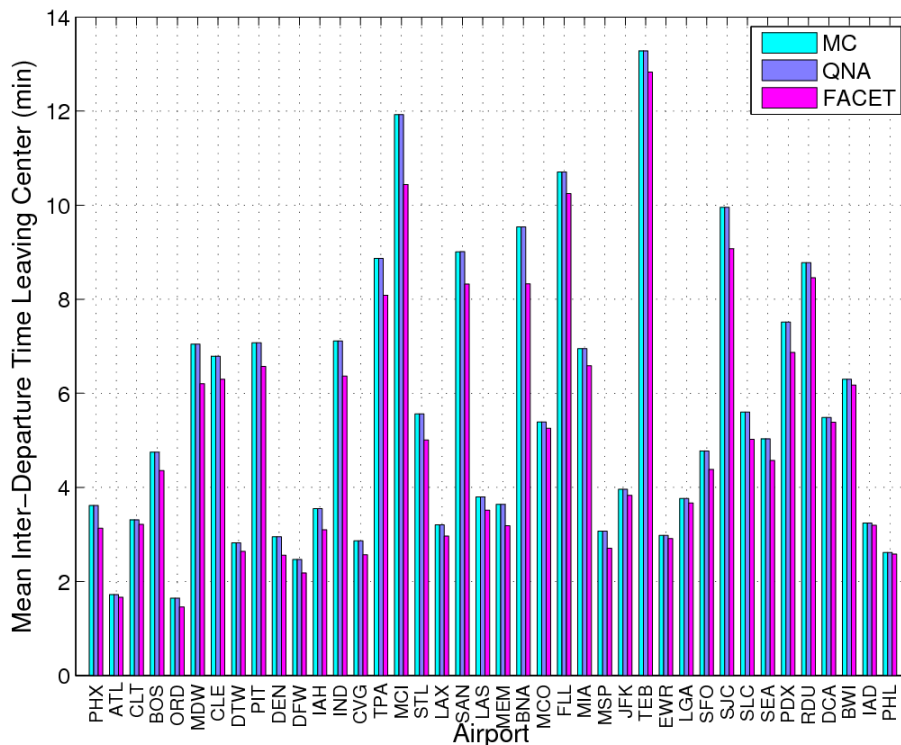


Figure 28. Mean Inter-Departure Times for Flows from Centers to Airports, from Monte Carlo Simulations, QNA Solution, and FACET

The results given in this section show that the QNA approach performs remarkably well in estimating the mean flow rates through the nodes of the queuing network. These values also compare very well with FACET. Since the computation of the mean values for the Jackson network is the same as the QNA approach, these remarks are equally valid for the Jackson network. Additional FACET runs will aid in getting more accurate values for comparison.

The QNA approach also calculates improved estimates of the standard deviation of the interval time of arriving and departing flows to within 10% accuracy in most cases. It is found that the mean number of aircraft in each node of the queuing network can be calculated to within 5% accuracy in almost all cases. However, the QNA solution appears to underestimate the standard deviation of the number of items in service. At the present time, this difference is attributed to the aggregation effects introduced by spatial discretization of the airspace.

## II. Conclusions

This paper discussed a framework for carrying out the stochastic analysis of the National Airspace system using multi-resolution queuing network models. The approach for using historic traffic data for formulating the queuing models was discussed, together with approaches for modeling the uncertainties in the National Airspace System. Although models for climb and descent have been derived in a companion paper, only the en-route uncertainty models were presented in this paper. NAS traffic flow characteristics were examined using both Jackson networks and QNA approximation based queuing networks. Due to the algebraic nature of these computations, these networks are useful for rapid trade studies, and for providing real-time strategic traffic flow decision support. The queuing models were validated using Monte Carlo simulations. It was shown that the queuing networks can predict the mean traffic flow within 5% of FACET simulations. Depending upon the spatial discretization employed, these networks were observed to underestimate the variance of the traffic flows.

All the algorithms derived under the present research have been implemented in a software package for modeling and analyzing queuing models of the NAS. This software package uses FACET air traffic simulations to

generate the data required for formulating the queuing models. Scriptable environments can be used in conjunction with this software package to formulate NAS queuing models at multiple spatial resolutions. Use of this software for developing decision support tools will be of future interest.

### Acknowledgments

This research was supported under NASA Contract No. NNA07BC55C, with Mr. Michael Bloem and Ms. Jane Thippavong as the Technical Monitors. Ms. Rebecca Grus served as the COTR. The authors would like to thank Mr. Bloem, Ms. Thippavong, Mr. Todd Farley, Dr. Shon Grabbe, Dr. Sridhar, Dr. Chatterji and several others at NASA for their interest and support of this research effort. Authors also thank Professors Jay Rosenberger and Kamesh Subbarao of the University of Texas at Arlington for their contribution to portions of this research.

### References

- <sup>1</sup>Bilimoria, K. D., Sridhar, B., Chatterji, G. B., Sheth, G., and Grabbe, S., "FACET: Future ATM Concepts Evaluation Tool," *3<sup>rd</sup> USA/Europe Air Traffic Management R&D Seminar*, Naples, Italy, June 2000.
- <sup>2</sup>Raytheon ATMSDI Team, "Airspace Concept Evaluation System Build 2 Software User Manual," NASA Ames Research Center, Moffett Field, CA, November 2003.
- <sup>3</sup>Saaty, T. L., *Elements of Queuing Theory with Applications*, Dover Publications, Inc., New York, NY, 1983.
- <sup>4</sup>Jackson, J. R., "Networks of Waiting Lines," *Operations Research*, Vol. 5, No. 4, August 1957, pp. 518-521.
- <sup>5</sup>Perros, H. G., *Queueing Networks with Blocking*, Oxford University Press, New York, NY, 1994, pp 15-30.
- <sup>6</sup>Whitt, W., "The Queuing Network Analyzer," *The Bell System Technical Journal*, Vol. 62, Issue No. 9, November 1983..
- <sup>7</sup>Erlang, A. K., "Solution of Some Probability Problems of Significance for Automatic Telephone Exchanges," *Elektrotekniker*, Vol. 13, pp. 5-13, 1917.
- <sup>8</sup>Pearcey, T., "Delay in Landing of Air Traffic," *Journal of the Royal Aeronautical Society*, Vol. 52, pp. 799-812, 1948.
- <sup>9</sup>Bell, G. E., "Operations Research into Air Traffic Control," *Journal of the Royal Aeronautical Society*, Vol. 53, pp. 965-978, 1949.
- <sup>10</sup>Bell, G. E., "Queueing Problems in Civil Aviation," *Operations Research Quarterly*, Vol. 3, pp. 9-11, 1952.
- <sup>11</sup>Long, D., Lee, D., Johnson, J., Gaier, E., and Kostiuik, P., "Modeling Air Traffic Management Technologies with a Queuing Network Model of the National Airspace System," NASA Contractor Report No. NASA-CR-1999-208988, January 1999.
- <sup>12</sup>Menon, P. K., Sweriduk, G. D., Lam, T., Cheng, V. H. L., and Bilimoria, K. D., "Air Traffic Flow Modeling, Analysis and Control," *AIAA Guidance, Navigation and Control Conference*, August 11-14, 2003, Austin, TX.
- <sup>13</sup>Menon, P. K., Sweriduk, G. D., and Bilimoria, K. D., "A New Approach for Modeling, Analysis and Control of Air Traffic Flow," *Journal of Guidance, Control and Dynamics*, Vol. 27, No. 4, 2004, pp. 737-744.
- <sup>14</sup>Menon, P. K., Sweriduk, G. D., Lam, T., Diaz, G. M., and Bilimoria, K. D., "Computer-aided Eulerian Air Traffic Flow Modeling and Predictive Control," *Journal of Guidance, Control and Dynamics*, Vol. 29, No. 1, January-February 2006, pp. 12-19.
- <sup>15</sup>Sridhar, B., Soni, T., Sheth, K. S., and Chatterji, G. B., "An Aggregate Flow Model for Air Traffic Management," *AIAA Guidance, Navigation and Control Conference*, August 16-19, 2004, Providence, RI.
- <sup>16</sup>Bayen, A., Raffard, R., Tomlin, C. "Eulerian Network Model of Air Traffic Flow in Congested Areas," *Proceedings of the 2004 American Control Conference*, June 2004.
- <sup>17</sup>Grabbe, S., Sridhar, B., "Congestion Management with an Aggregate Flow Model," *AIAA Guidance, Navigation and Control Conference*, August 15-18, 2005, San Francisco, CA.
- <sup>18</sup>Fredrick S. Hillier and Gerald J. Lieberman, *Introduction to Operations Research*, McGraw-Hill, New York, NY, 2001.
- <sup>19</sup>Cassandras, C. G., and Lafortune, S., *Introduction to Discrete Event Systems*, Kluwer Academic Publishers, Boston, MA, 1999.
- <sup>20</sup>Kim, J., Palaniappan, K., Menon, P. K., Subbarao, K., and Nag, M., "Trajectory Uncertainty Modeling for Queueing Analysis of the NAS," *AIAA Aviation Technology, Integration, and Operations Conference*, Anchorage, AK, September 2008.
- <sup>21</sup>Gelb, A., *Applied Optimal Estimation*, The M.I.T. Press, 1979.
- <sup>22</sup>Kayton, M. and Fried, W. R. *Avionics Navigation Systems*, John Wiley & Sons, Inc., 1997.
- <sup>23</sup>RNP Capability of FMC Equipped 737, Generation 3, D6-39067-3, The Boeing Company, 2005.
- <sup>24</sup>Beichelt, F., *Stochastic Processes in Science, Engineering and Finance*, Chapman & Hall/CRC, 2006.
- <sup>25</sup>Simon, M. K., *Probability Distributions Involving Gaussian Random Variables, A Handbook for Engineers, Scientists and Mathematicians*, Springer, 2006.

<sup>26</sup> Tandale, M.D., Sengupta, P., Menon, P. K., Cheng, V. H. L., Rosenberger, J., and Subbarao, K., "Queuing Network Models of the National Airspace System," *8<sup>th</sup> AIAA Aviation Technology, Integration, and Operation (ATIO) Conference*, September 14-19, 2008, Anchorage, AK.

<sup>27</sup> System-Wide Concept Report, Virtual Airspace Modeling and Simulation Project, *VAMS Project Office NASA Ames Research Center*, Vol. 3, Appendices, June 23, 2006.